

Investigating sensitivity of ozone to emission reductions in the New York City (NYC) metropolitan and downwind areas

Trang Tran ^{a,*}, Naresh Kumar ^a, Eladio Knipping ^b

^a Desert Research Institute, Division of Atmospheric Sciences, 2215 Raggio Parkway, Reno, NV, 89512, USA

^b Electric Power Research Institute, 1325 G St. NW Suite 530, Washington, DC, 20005, USA



HIGHLIGHTS

- We examine ozone sensitivity to emission changes in NYC using WRF-CAMx.
- Large positive wind biases were reduced using observational nudging.
- NYC was shown to be VOC-limited ozone formation regime.
- Reducing man-made emissions by 50% significantly improved ozone concentrations.
- Ozone production efficiency increased when emissions decreased.

ARTICLE INFO

Keywords:

WRF
CAMx
Ozone
NYC
LISTOS
Source apportionment

ABSTRACT

Ozone sensitivity to emission changes in urban environments were examined using WRF and CAMx simulations for the New York City metropolitan area (NYC) with data from the 2018 Long Island Sound Tropospheric Ozone Study measurements. The WRF simulation showed large positive biases of windspeed over entire domain, but those were significantly reduced with observational nudging. The base CAMx simulation showed large positive bias for NO₂ concentrations in NYC, which was corrected after NO_x emission adjustment (22% reduction) based on previous work. The improved modeling platform demonstrated reliable performance skills for regulatory applications. Pollution transport from NYC to the downwind region were well captured by the model. Simulated ozone concentration increases in response to NO_x emission reductions within NYC proximity suggested this area to be a VOC-limited ozone formation regime. Reducing anthropogenic emissions by 50% for all pollutants reduced the number of simulated ozone exceedances from 18 to 9 days for NYC. Emission reductions were even more effective for air quality improvements in the downwind region with ozone exceedances decreasing from 20 to 7 days. Source apportionment showed mobile and industrial solvent emission sectors to be contributing more to ozone exceedances than the electrical generating units (EGU) sector in both NYC and the downwind region. The largest air quality improvement appeared to be associated with VOC emission reductions from the industrial solvent sector. All source sectors yielded higher ozone production efficiency when emissions were reduced by 50%, suggesting remaining emissions can be more potent in producing ozone per molecule of NO_x.

1. Introduction

Tropospheric ozone (O₃) is one of six criteria pollutants for which the United States Environmental Protection Agency (EPA) has established National Ambient Air Quality Standards (NAAQS). O₃ is not directly emitted but is rather photochemically formed by two main precursor groups: nitrogen oxides (NO_x = NO + NO₂) and volatile organic compounds (VOC) (Jacob, 1999; Seinfeld and Pandis, 2016). Elevated ozone

concentrations are often observed in urban environments during hot summer months because two required ingredients become available for ozone formation: strong solar radiation and abundant precursors emitted from sources such as vehicles, power plants, industrial boilers, refineries, and chemical plants. Emissions of NO_x and VOC have decreased significantly by 64% and 23%, respectively, in the U.S. over the last 2 decades (Xing et al., 2013; Nopmongcol et al., 2016; EPA, 2022); however, ozone concentrations in urban areas have not

* Corresponding author.

E-mail address: trang.tran@dri.edu (T. Tran).

decreased to the same degree (Simon et al., 2015; EPA, 2020) due to the non-linear relationship between ozone and precursors concentrations. Many of the major metropolitan areas along U.S. coasts are still classified as ozone nonattainment areas as of March 2022 (EPA Greenbook, 2022) including both the West Coast (e.g., Los Angeles-South Coast Air Basin (severe); San Francisco Bay Area (marginal)) and the East Coast (e.g., New York – Northern New Jersey – Long Island, NY-NJ-CT (moderate); Philadelphia-Wilmington Atlantic City (marginal), PA-NJ-MD-DE (marginal) and Washington, DC-MD-VA (marginal)). To meet or maintain attainment of current and future ozone NAAQS in these areas, it is critical to understand the sensitivity of ozone concentrations to emissions from various sources.

Nopmongcol et al. (2017) used the Comprehensive Air Quality Model with Extensions (CAMx) Source Apportionment Technology to estimate contributions to O₃ and PM_{2.5} from 6 source sectors in 7 source regions in the U.S. from 1970 to 2020. They found that NOx and VOC emissions have decreased significantly over the years leading to lower O₃ concentrations. However, decreases in NOx emissions raised O₃ production efficiency (OPE) across all emission categories, which raises questions about benefits of further NOx emissions reductions to control ozone. Therefore, it is important to further understand the OPE in different areas, as that may shed light on how ozone concentrations may respond to further emission reductions.

Among the various nonattainment areas, the NY-NJ-CT area has drawn much regulatory and research attention due to: i) high population density, ii) persistent ozone exceedances during summer months and a recent flattened trend in ozone concentrations instead of decreasing trend (EPA, 2020). A recent multi-agency collaborative study named Long Island Sound Tropospheric Ozone Study (LISTOS) was initiated by the Northeast States for Coordinated Air Use Management (NESCAUM) (LISTOS: <https://www.nescaum.org/documents/listos>) to better understand ozone formation and transport from New York City metropolitan area (NYC) to downwind areas including Long Island Sound (LIS) and shorelines of downwind states (e.g., Connecticut) (Karambelas, 2020). The summer 2018 LISTOS monitoring campaign included various types of measurements made by mobile labs, aircraft, satellite measurements, and ground-based stations to understand how land–water interactions influence O₃ concentrations (Moshary et al., 2020; Wu et al., 2021; Zhang et al., 2021; Zhao et al., 2020). Observations revealed the presence of a low-level jet off the Connecticut shoreline associated with ozone events (Karambelas, 2020). LISTOS stakeholders have indicated a need of chemical transport models (CTMs) that can replicate such weather conditions and the ozone concentration distribution to support the state implementation plans in the Northeast. Ma et al. (2021) and Torres-Vazquez et al. (2022) have made use of observations to develop CTM configurations and modifications that improve model performance in simulating meteorological and chemical fields in the LISTOS area. All of these data and analysis make LISTOS well-served for a case study to investigate ozone sensitivity to emission reductions.

Although previous LISTOS modeling studies (Ma et al., 2021; Torres-Vazquez et al., 2022) have developed improved CTM modeling configurations, those studies focus more on performance sensitivity experiments as part of an initial phase of model development for regulatory use. A study evaluating the air quality model for regulatory applications and addressing ozone sensitivity to emission changes is still lacking. This study aims to leverage observations and previously available model inputs to simulate ozone chemistry in the NYC metropolitan area to examine the response of ozone concentrations to emissions reductions and assist decisions on emission control strategies. The findings from this study can guide applications in other similar ozone non-attainment urban areas. The objectives of this study include:

- 1) Conducting a model performance evaluation (MPE) for base simulations using the “default” WRF and CAMx model inputs leveraged from LISTOS modeling studies. MPE followed EPA’s (2018)

operational approach recommended for model testing for air quality planning purposes

- 2) Optimizing model performance using data assimilation and emissions adjustment and demonstrating improved model performance based on commonly used benchmarks;
- 3) Examining ozone sensitivity to emission changes by different source sectors using source apportionment techniques.
- 4) Determining changes in OPE as emissions from different sectors change.

2. Methodology

CAMx version 7.0 (Ramboll, 2020) was used to conduct the base case and source apportionment modeling in LISTOS on a 1.33 km gridded resolution domain. Gas phase chemistry used the Carbon Bond Version 6 (CB6r4) mechanism, which was originally developed for summer ozone chemistry in urban environments (Gery et al., 1989; Yarwood et al., 2005, 2010). Compared to previous versions, CB6r4 explicitly adds some long-lived organics that form ozone at regional scales, such as propane, benzene, acetone, and ketones (Yarwood et al., 2010). Horizontal and vertical transport were configured with Eddy diffusivity scheme and Piecewise Parabolic Method (Colella and Woodward (1984)) advection scheme. Dry deposition followed Zhang et al.’s (2003) approach utilizing 23 landuse categories. Meteorological input data for CAMx were developed using the Weather Forecasting and Research (WRF; Skamarock et al., 2019) model nudged toward North American Model (NAM) 12-km analyses and the Meteorological Assimilation Data Ingest System (MADIS) observations. Meteorological conditions were extracted from WRF outputs by WRFCAMX Version 4.8.1 tool for CAMx domain aligning with WRF domain excluding six lateral boundary grids. Lateral boundary conditions were provided by the EPA Office of Research and Development (EPA-ORD). WRF-CAMx simulations were performed over the LISTOS studied period of May 2 – September 30, 2018, to leverage EPA-ORD’s model inputs as well as observational data collected by other research groups during this time. The statistical models of Camalier et al. (2007) and Wells et al. (2021) indicate that summer ozone is more readily formed on warm, calm and sunny days. The unique atmospheric physics of chronic ozone problems in NYC and downwind regions is polluted air masses being transported in northeast direction out of NYC over Long Island Sound (LIS). The relatively cool waters of LIS confine the pollutants in a shallow and stable marine boundary layer. Afternoon heating over coastal land creates a sea breeze that carries the air pollution inland from the confined marine layer, resulting in high ozone concentrations in NYC downwind shorelines. Zhang et al. (2021) indicated that multiple heatwave episodes and significant marine air flow influences occurred in summer 2018 in NYC and LIS areas, which are representative for typical atmospheric physics associated with ozone exceedances in the area.

2.1. Meteorological model description

Weather conditions were simulated using the WRF model on a 1.33 km gridded resolution domain (Fig. 1) which is identical to the finest 1.33 km-resolution domain in EPA-ORD LISTOS modeling platform. This domain includes a 318 × 348 horizontal grid and 36 vertical layers extending from the surface to 20 km above ground level (AGL) (Torres-Vazquez et al., 2022). The first km AGL is represented by 14 layers with a 20 m height for the lowest layer. Initial and boundary conditions (IC/BC) were obtained from LISTOS EPA-ORD model outputs produced on a 4 km-resolution outer domain (*per. comm.*) using 1-way nesting.

WRF Version 4.2 configurations were based upon those well tested for simulating weather conditions in urban environments (Appel et al., 2014; Ran et al., 2016; Torres-Vazquez et al., 2022). The Morrison double-moment microphysics scheme simulated double-moment ice, snow, rain and graupel at cloud-resolving resolution (Morrison et al., 2005). Cumulus convection was resolved by the simulations because of

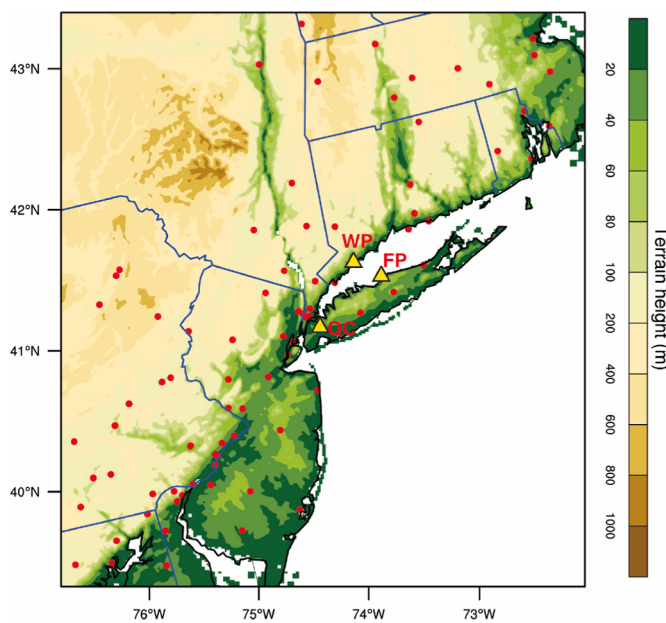


Fig. 1. WRF-CAMx modeling domain. Red dots indicate Air Quality System (AQS) monitoring stations used for calculating model performance statistics. Triangles indicate Queens College (QC), Westport (WP) and Flax Pond (FP) sites used for in-depth analysis.

the fine grid scale of 1.33 km. The treatment of long-wave and short-wave radiation was based on Iacono et al. (2008)'s Rapid Radiative Transfer Model. The Pleim-Xiu land surface model (LSM) (Pleim and Xiu, 1995; Xiu and Pleim, 2001) was chosen to apply soil nudging where observational ground level temperature and water vapor mixing ratio are utilized for deep soil moisture and temperature nudging (Pleim and Gilliam, 2015). Pleim-Xiu surface physics and Asymmetric Convective Model (ACM2) boundary layer scheme were used as compatible physics schemes with the selected LSM to calculate atmospheric turbulence. Analysis nudging of temperature, water mixing ratio, zonal and meridional wind components was applied above the planetary boundary layer using North American Model 12 km analysis on a 3-hr basis.

2.2. Emissions

Emission input files were obtained from EPA-ORD. Details of emission data are described by Torres-Vazquez et al. (2022). In summary, anthropogenic emissions were based on National Emission Inventory (NEI) Version 7.2 of the 2016 beta modeling platform (EPA, 2019) with updates made for several sectors, as described subsequently. This emission modeling platform is a product of the National Emissions Inventory Collaborative - a collaboration of state and regional air agencies, EPA, and Federal Land Management agencies and includes a full suite of base year 2016 inventories, ancillary emission data, and scripts and software for preparing the emissions for air quality modeling. Fire and electric generating units (EGU) point emissions were prepared using 2018-year specific input data. EGU and other point source emissions with stack heights larger than 20m were treated as elevated sources. EGU units that are matched with the Continuous Emissions Monitoring System (CEMS) data vary with high demand during heat-wave days. For sources not matched to CEMS units, the allocation of the inventory annual emissions to months is done using average fuel-specific annual-to-month factors generated for regions with similar climate. Emissions were allocated from month to day using the Integrated Planning Model (IPM)-region and fuel-specific average month-to-day factors also based on the 2016 CEMS heat data (EPA, 2019). On-road and non-road mobile emissions were processed for 2018 from a Sparse Matrix Operator Kernel Emissions - Motor Vehicle Emission Simulator

(SMOKE-MOVES) simulation with county-level 2016 inputs and year-to-year adjustment factor. Updates included in a newer NEI version (e.g., 2017 platform) for airport emissions and commercial marine vessels were applied for 2018 emission projection. Industrial solvents were treated separately from other area emission sectors by Torres-Vazquez et al. (2022) following Seltzer et al. (2021). NEI emissions were processed into CAMx-ready format at 1.33 km grid resolution. Total emissions for NO_x and VOC over entire domains were approximately 207,475 tons nitrogen and 2,675,811 tons carbon, respectively, per month.

Biogenic VOC emissions and soil NO_x emissions were computed using the Biogenic Emission Inventory System (BEIS3.61; Bash et al., 2016) within the SMOKE model and with the WRF's meteorological variables processed by the Meteorology-Chemistry Interface Processor (MCIP) to maintain the consistency with Torres-Vazquez et al.'s in-line calculation for biogenic emissions. The Biogenic Emissions Landuse Database version 4.1 (BELD4; last updated February 2017) was processed with the Spatial Allocator Version 4.3.2 (<https://github.com/CMASSCenter/Spatial-Allocator>) tool to provide inputs for BEIS.

Other natural sources such as windblown dust, oceanic aerosol, and lightning were prepared by WBDUST, OCEANIC, and LNOX preprocessors (Ramboll, 2020), respectively, then merged into the EPA-ORD emissions. In-line oceanic inorganic iodine emissions were calculated internally by CAMx to account for ozone depletion related to this group of compounds in the coastal marine boundary layer (Ramboll, 2020).

Fig. 2 shows domain-wide distributions of column-summed hourly average NO_x (left) and VOC (right) emissions from all anthropogenic sources as well as biogenic sources. The New York City metropolitan area (NYC) stands out from other regions due to the remarkably higher anthropogenic NO_x and VOC emissions. Emissions over LIS and the shorelines of the downstream states (e.g., Connecticut, Rhode Island) were noticeably lower than NYC. Biogenic NO_x emissions were extremely small (e.g., less than 1%) in comparison with anthropogenic NO_x emissions over entire domain (Fig. 2a and b). Domain-average VOC biogenic emissions were 4.4 times higher than anthropogenic emissions. However, most of high biogenic emissions happened in sub-urban or rural areas such as (Fig. 2b). In NYC (e.g., Queens College) and its downwind areas (e.g., Westport), anthropogenic emissions were about 6.7 and 1.2 times higher than biogenic emissions, respectively.

2.3. Analysis method and observational data

This study analysis focused on: 1) model performance evaluation (MPE) for WRF and CAMx simulations using the "default" (or base) EPA-ORD emission inputs; 2) optimizing performance by data assimilation and emission adjustments; and 3) examining ozone sensitivity to emission changes per sector using source apportionment.

MPE including statistical and graphic analysis was performed for all simulations following EPA's (2018) guidance for regulatory applications for air quality models. The Atmospheric Model Evaluation Tool (AMET) developed by Appel et al. (2013) and other plotting tools were used for MPE. Calculated statistic metrics were compared to sets of standard model performance benchmarks developed through an extensive review of various modeling studies (Bowden and TalgoAdelman, 2016; Kemball-Cook et al., 2005; McNally, 2009; Simon et al., 2012; Emery et al., 2017). Domain-wide averaged as well as station data were examined. The Queens College (substituted by Flax Pond for vertical profiles) and Westport monitoring sites (Fig. 1) were chosen to demonstrate pollution transport from NYC downwind because of their vicinity to NYC and observation availability.

Ozone sensitivity to emission changes was assessed by source apportionment analysis for the base and optimized scenarios. Source contributions were calculated for maximum daily 8-h average ozone concentrations (MDA8-O₃) on days exceeding NAAQS of 70 ppb. OPE defined as the number of O₃ molecules formed for every molecule of

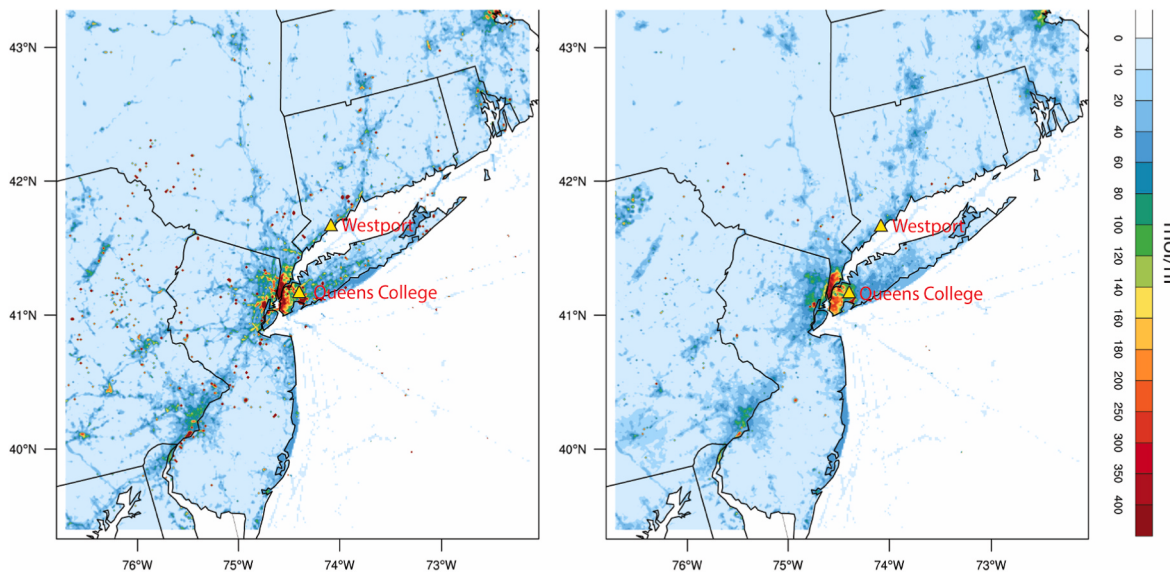


Fig. 2a. Hourly NOx (left) and non-methane VOC anthropogenic emissions (right) averaged over entire modeling period. Triangles indicate locations of sites of interest.

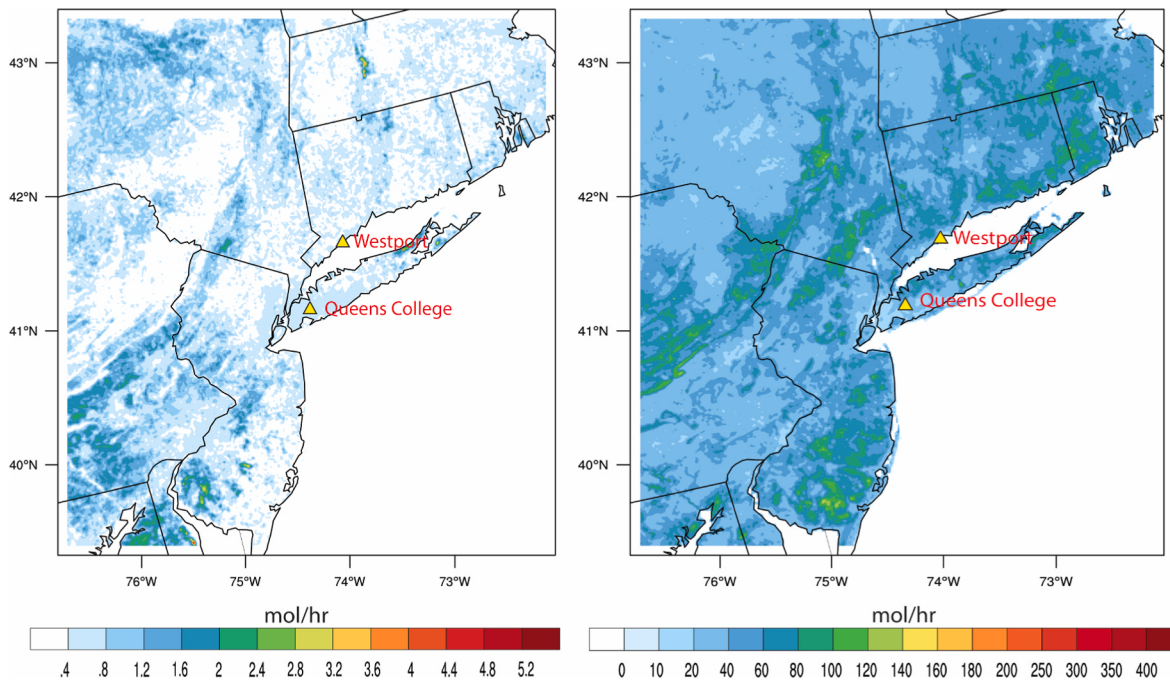


Fig. 2b. Hourly NO (left) and non-methane VOC biogenic emissions (right) average over entire modeling period. Triangles indicate locations of sites of interest.

NO_x oxidized (Liu et al., 1987) were assessed for total emissions as well as NO_x-dominant emission sectors (e.g., mobile, EGU). It is important to understand the OPE in different areas, as that may shed light into how ozone concentrations may respond to further emission reductions. OPE was calculated as slope of the linear regression between hourly odd oxygen ($\text{Ox} = \text{O}_3 + \text{NO}_2$) versus oxidized nitrogen reservoir species (e.g., NO₂ including gaseous nitric acid, peroxyacetyl nitrate, peroxy nitric acid and organic nitrates) following the methodology of prior studies (Kleinman et al., 2002; Ninneman et al., 2017; Hembeck et al., 2019) for surface layer. Coefficients of determination (r^2) for Ox versus NO₂ concentrations were also calculated.

Observational data used in this study were obtained from MADIS (<https://madis.ncep.noaa.gov/>), EPA's Air Quality System (AQS, <http://www.epa.gov/aqs>), and other data across the NYC and LIS areas

collected during LISTOS measurement campaign in summer 2018 (<https://www-air.larc.nasa.gov/missions/listos/index.html>).

3. Model performance

We started with the base simulation using model inputs received from EPA ORD and then performed successive sensitivity tests on both WRF and CAMx to optimize model performance before conducting the emission sensitivity simulation.

3.1. WRF model performance

We first conducted model performance on the WRF simulation using the same configuration as EPA ORD (referred to as BASE simulation).

The BASE model performance evaluation (MPE) showed a high degree of agreement between modeled and observed surface temperature and water mixing ratio (Fig. 3, top), consistent with Torres-Vazquez et al.'s MPE. However, WRF yielded larger errors in simulating the surface wind field over MADIS meteorological monitoring stations (Fig. 3, bottom). These errors appear to be high in comparison with Torres-Vazquez et al.'s MPE despite the shared model configurations. These differences stem from the different regions of interest. Our study looked at domain-wide average values while Torres-Vazquez et al. focused on a much smaller region of interest centered in the NYC-LIS area. Surface wind-speed overestimation produced by WRF is a well-known issue especially in the coastal area as previously discussed in different studies (Powell et al., 2003; Ngan et al., 2013; Misaki et al., 2019) with the most likely cause being that the model misrepresents the high spatial variability of the wind field under the effects of thermal atmospheric gradients between land and water bodies.

The BASE simulation captured the temporal evolution of surface meteorological quantities averaged over the entire domain throughout the studied period except for wind speed (Fig. 4, red versus black lines). The strong overestimation of wind speed predicted by WRF could potentially lead to erroneous distribution of pollutants at different locations; therefore, it is crucial to address such biases before the model is used for emission control sensitivity experiments. We applied observational nudging (Reen, 2016) to surface winds to improve model performance using the MADIS database because this technique has proven to reduce model biases for surface meteorology (Reen and Dumais, 2014; Tran et al., 2018). Different nudging coefficients (nudging strengths: 4×10^{-4} ; 6×10^{-4} and 64×10^{-4}), which determines how strongly and quickly simulated terms approach the observed values were tested to determine the optimum coefficient to be the largest coefficient of 64×10^{-4} that yielded the most significant model performance improvement while still retained meteorologically consistent solutions in model calculations. The radius of influence was set to 50 km. The nudging time window was set to 40 min so that nudging starts and ends its influence within 1 h. This simulation with observational nudging is referred to as the NUDGE simulation.

Throughout the entire simulation period, surface wind observational nudging reduced model errors for wind speed and improved performance for wind direction while it did not affect WRF's ability in simulating temperature and water mixing ratio (Fig. 4). AMET-derived mean absolute error (MAE) of the NUDGE simulation was about two times smaller than the BASE simulation for wind direction (e.g., MAE reduced from 23.4 to 12.3) and five times smaller for wind speed (e.g., MAE reduced from 1.1 to 0.2) (Fig. 4). Wind direction improves to a lesser extent than wind speed improvement after nudging application because this quantity was already predicted relatively well without nudging as shown in Fig. 4 (bottom panel, black vs red lines). Index of Agreement (IOA) of wind speed simulated by the NUDGE simulation increased (0.82) compared to the BASE simulation (0.65)..

Both the BASE and NUDGE WRF simulations reproduced vertical temperature profiles for both night/early morning and mid-afternoon hours at Flax Pond, the station closer to NYC source region (Fig. 5a), and at Westport downwind (Fig. 5b). The stable/neutral conditions within a shallow boundary layer (~ 250 m) during night/early morning time were captured at both locations. Well-mixed conditions during afternoon were also simulated correctly. The model performed reasonably well in simulating humidity throughout the first 1.5 km above ground level (AGL). The model was able to capture low level jets (below 500 m AGL) at both locations for three out of four sonde comparisons.

The NUDGE simulation with surface observational wind nudging barely affected the model's ability in simulating temperature and RH profiles but consistently improved the model performance for wind speed profiles within 200m AGL at both locations (Fig. 5a and b).

Table 1 shows the final performance metrics for the WRF NUDGE simulation. The WRF simulation passed all the commonly accepted performance benchmark criteria following Bowden and TalgoAdelman

(2016) through an extensive review of relevant studies (Emery et al., 2001; Kemball-Cook et al., 2005; McNally, 2009).

With the improvements introduced into model performance by surface wind nudging, the NUDGE simulation results were chosen to provide meteorological fields to drive the CAMx simulations.

3.2. CAMx model performance

Temporal evolution of maximum daily 8-h average ozone (MDA8-O₃) concentrations throughout the entire summer were well replicated when CAMx was run for the NUDGE case (i.e., using the WRF results from the NUDGE simulation) (Fig. 6, red versus black line) at both Queens College site in NYC source region and Westport site in the downwind region. For simplicity we will continue to refer to this as the NUDGE simulation for CAMx as well. The NUDGE simulation was able to predict the exceedance timing although overestimating the magnitude of some exceedances in August by up to 20 ppb. The NUDGE simulation performance worsened in September when ozone concentrations were low compared to the previous summer months, although WRF performance for weather conditions in September had remained comparable with the other months (Table 1).

The NUDGE simulation captured the diurnal cycle of ozone concentrations at Queen College (Fig. 7, top-left) with an overestimation and underestimation of 10 ppb during mid-afternoon and rush hours (i.e., early morning and late afternoon), respectively. The underestimation of ozone during rush hours at Queens College coincided with overestimation of NO₂ peaks (Fig. 7, bottom-left), suggesting that mobile source NO_x emissions in the NYC source region might be overestimated for these time intervals. The NUDGE simulation performed worse at the Westport site than at the Queens College with respect to the ozone diurnal cycle with positive biases throughout the day except for the hours between 6 and 11 a.m. local time when the model results agreed well with observations (Fig. 7, top-right). Westport is downwind from NYC where pollutant concentrations were affected by both local emissions and pollution transport from the upwind source region; therefore, the observed NO₂ diurnal variations were not necessarily reflected in the ozone diurnal pattern. The model, however, still predicted maxima and minima of NO₂ coinciding with minima and maxima of O₃, respectively (Fig. 7, bottom-right). Despite the unrepresentative simulated NO₂ diurnal pattern, the relatively low NO₂ concentrations at Westport compared to Queens College were captured by the model, suggesting reasonable NO_x emission estimates for this downwind area.

Similar to the NO₂ model performance, the model reproduced hourly formaldehyde concentrations within the observed ranges although the model often underestimated some peaks by 2 ppb (Fig. 8, top). The timing of high and low formaldehyde episodes was also simulated correctly throughout the entire summer.. The observed afternoon peak of formaldehyde concentrations is likely associated with the prompt oxidation of biogenic isoprene emissions (Wolfe et al., 2016), which peaks in the afternoon when foliage temperatures are highest. Despite the fact that BEIS biogenic emission model accounts for high afternoon peak of isoprene emissions (Schwede et al., 2005), CAMx failed to capture distinct formaldehyde day-night patterns (Fig. 8, bottom). Westport is strongly impacted by transports from its upwind NYC source region, therefore, the model inability in simulating formaldehyde concentration at this site could be more likely due to a combination of various model uncertainties rather than just emission errors.

Given the overpredictions of NO₂ concentrations at Queens College in NYC that likely also impact ozone model performance, and evidence from previous work (Goldberg et al., 2019) suggesting that the 2018 NEI NO_x emissions within 50 km radius from the NYC city center NYC were overestimated by 22% (based on the TROPOMI satellite-derived emissions), we conducted a performance sensitivity simulation with a 22% reduction of NO_x anthropogenic emissions within 50 km radius from the center of NYC (this simulation will be referred to as the REF simulation). Domain-wide natural emissions and anthropogenic emissions beyond

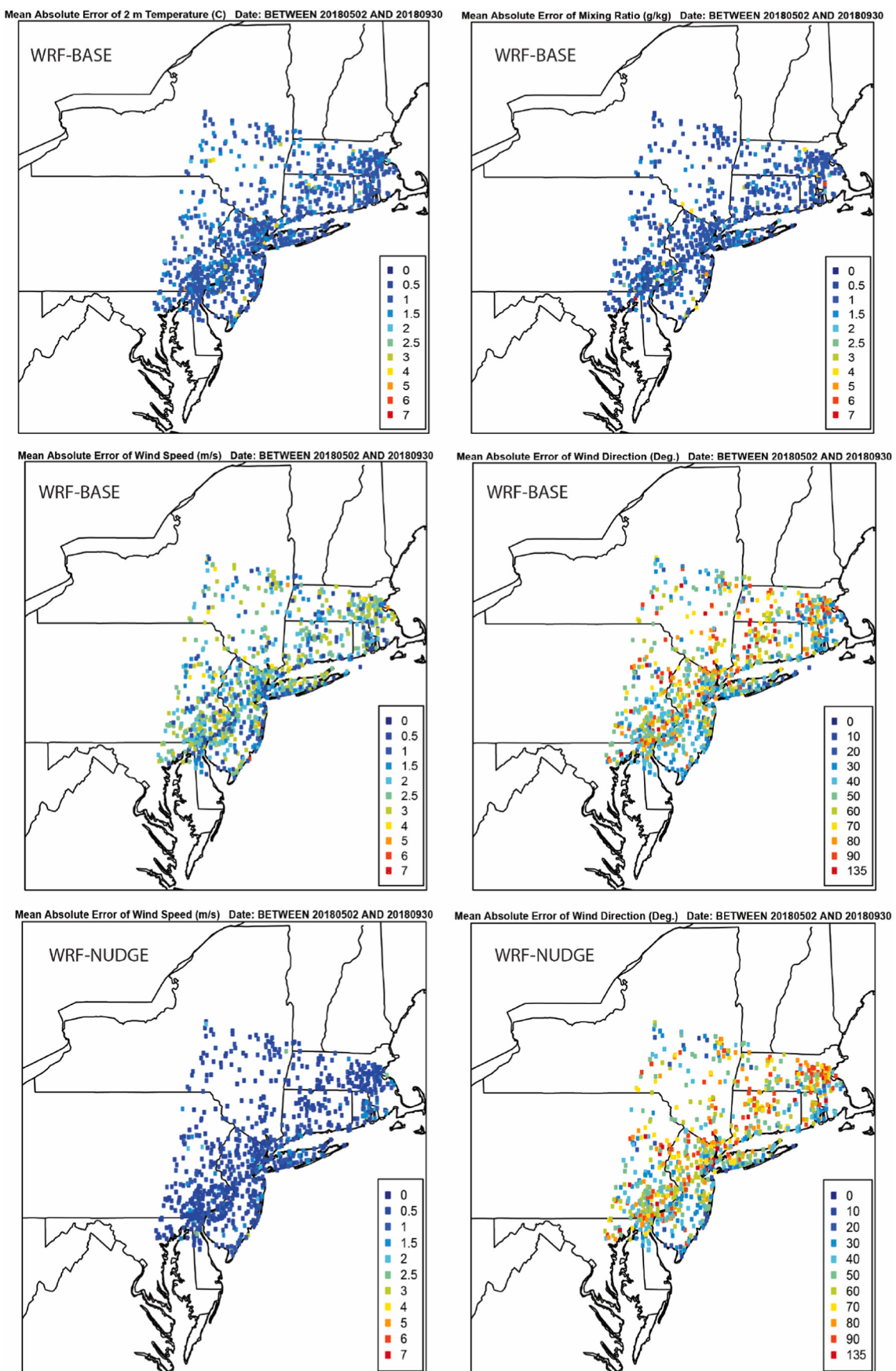


Fig. 3. Mean Absolute Error of conventional surface meteorological fields produced by WRF-BASE and WRF-NUDGE at MADIS monitoring stations. Data were averaged over entire modeling period.

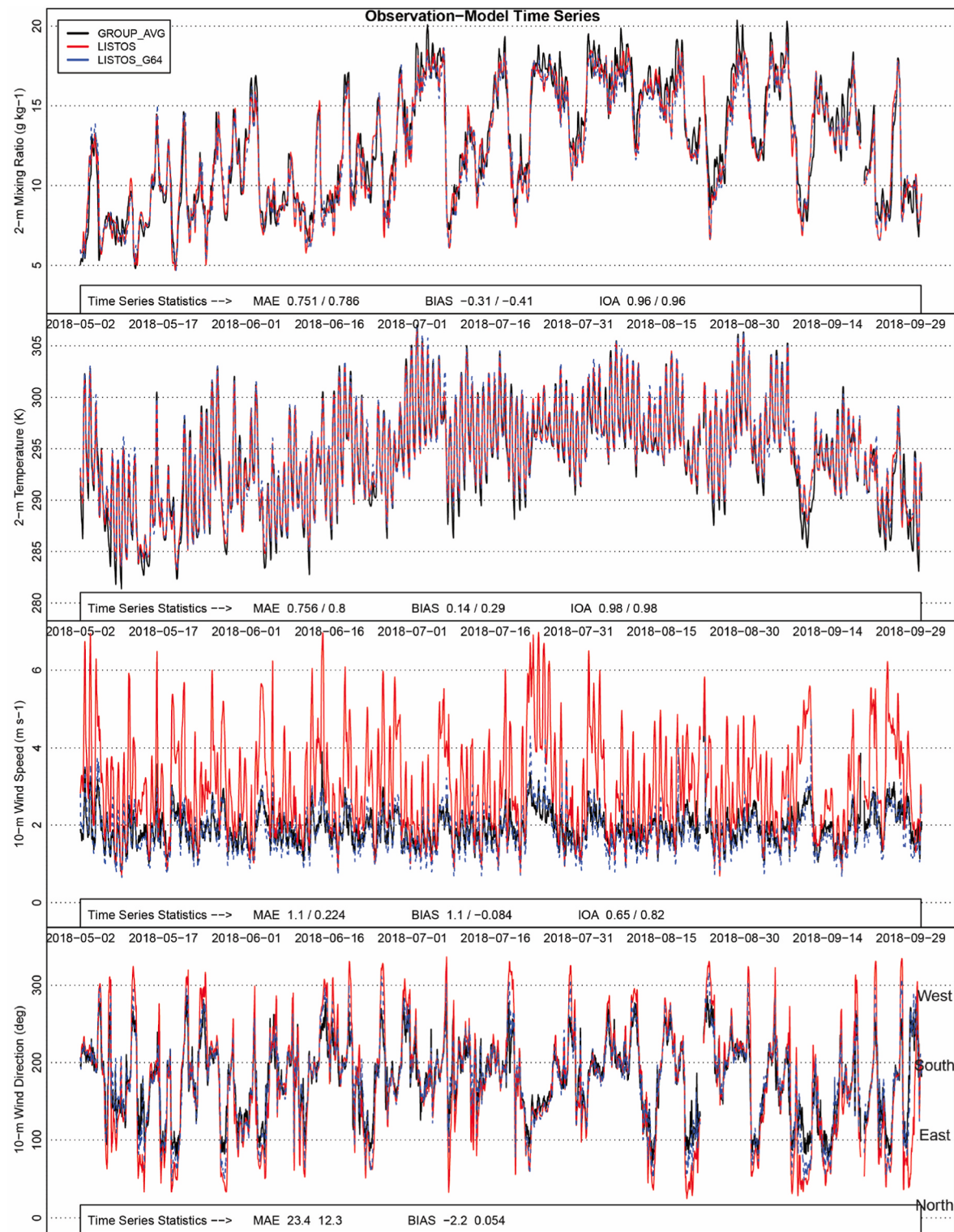


Fig. 4. Temporal evolutions of surface conventional meteorological fields as simulated by WRF-BASE (red), WRF-NUUDGE (blue) and observed (black). Data were average over all MADIS sites.

the 50 km radius were kept unchanged due to: i) Goldberg et al.'s TROPOMI satellite retrievals were limited within 50 km radius from NYC center and ii) while NUDGE simulations overestimated NO₂ concentrations at site in NYC (e.g. Queens College), the model reasonably replicated NO₂ concentration range at site in downwind region (e.g., West Port).

Lowering NOx emissions in the NYC area by 22% noticeably reduced

the NO₂ model biases at Queens College (Fig. 7 – bottom left). Reducing NO₂ emissions by 22% slightly increased ozone concentration at Queens College (Fig. 7, top left), indicating the NYC area to be in a VOC-limited ozone formation regime. The impact of emission adjustment on ozone and its precursors at the downwind Westport site were negligible (Fig. 7, right panels).

Because of the improvement made to model performance in

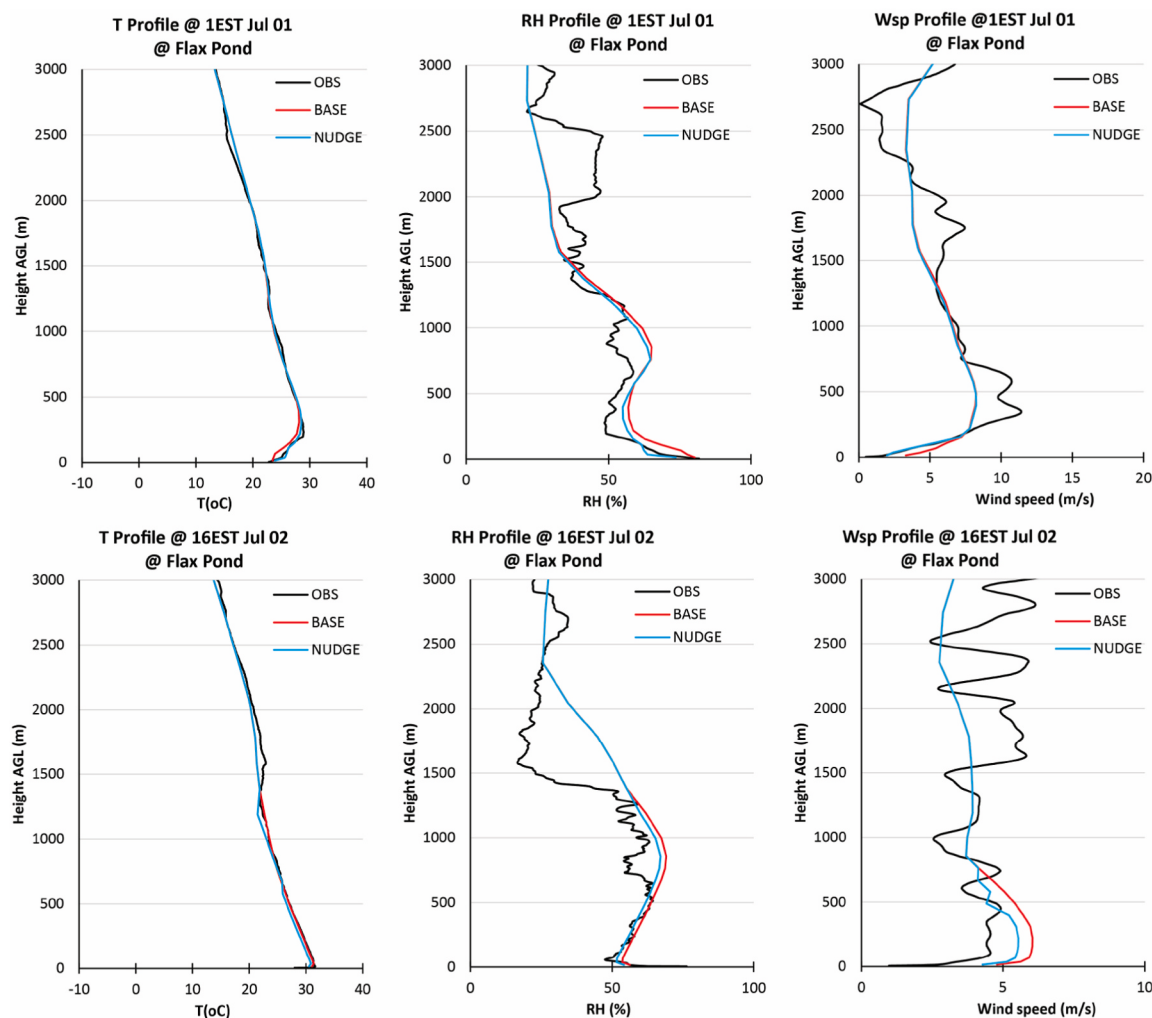


Fig. 5a. Vertical temperature (T), relative humidity (RH) and windspeed (Wsp) simulated by BASE (red) and NUDGE (blue) in comparison with ozonesonde-observed (black) data for nighttime (top panels) and mid-afternoon (bottom panels) at Flax Pond. Data were made available to public access at <https://www-air.larc.nasa.gov/missions/listos/index.html> by Professor Everette Joseph, University at Albany.

simulating surface NO₂ concentrations in NYC source region, emissions in REF (i.e., 22% reduced NOx emissions from default emissions prepared by EPA) simulation were chosen for this study as the final reference case.

Table 2 shows model performance for ozone for the REF simulation. For MDA8 ozone concentrations, correlation coefficients passed the “goal” benchmark of commonly accepted good performance recommended by Emery et al. (2017). The other performance scores passed “criteria” benchmark of acceptable performance except that August NMB of 18% slightly missed the threshold of 15%. September model performance was lower compared to other months although correlation coefficient still achieved performance goal. The overall statistical performance scores suggested reliable model performance for the REF simulation, thus indicating its suitability for conducting emission control sensitivity tests.

Spatial distributions of observed MDA8 ozone concentrations were replicated by the REF simulation for both non-exceedance and exceedance days (Fig. 9a). Torres-Vazquez et al. (2022) which shared almost identical WRF configurations and input data with this study showed that WRF was able to replicate the predominantly southwesterly (SW) flows in NYC-LIS region that prevailed throughout most of high ozone days. These typical SW pollution transport patterns - carrying ozone and its precursors from NYC to LIS, sequentially to Connecticut and occasionally ending at Rhode Island and Massachusetts - were demonstrated in

spatial distribution of MDA8-O₃ simulated by REF on exceedance days.

The ratios of simulated surface-HCHO to NO₂ concentration at NYC urban core were less than 2 (Fig. 9b), serving as strong indicator of VOC-limited ozone formation region according to Jin et al.’s (2020) identifications derived from multi-satellite HCHO/NO₂ records from 1996 to 2016 for NYC. Recent study by Tao et al. (2022) compiling observational data from satellite and aircraft measurements also revealed that ozone formation regime in center core of NYC to be VOC-limited for summer 2018. Our model-based and Tao et al.’s (2022) observational-based analysis also agree that the ozone formation regime shifted gradually from VOC-limited to transition and eventually to NOx-limited regime moving away from the city core center.

4. Result and discussion

4.1. Source contributions and ozone production efficiency

Ozone exceedances defined as events during which the MDA8-O₃ concentrations exceeding the 70 ppb NAAQS in the REF simulation were selected to quantify source contributions. The REF simulation identified 4, 6, and 8 exceedances occurring at Queens College in June, July and August, respectively, matching with observed exceedance timing (Fig. 6). Despite the location further away from NYC (Fig. 2), Westport was simulated to experience more ozone exceedances than Queens

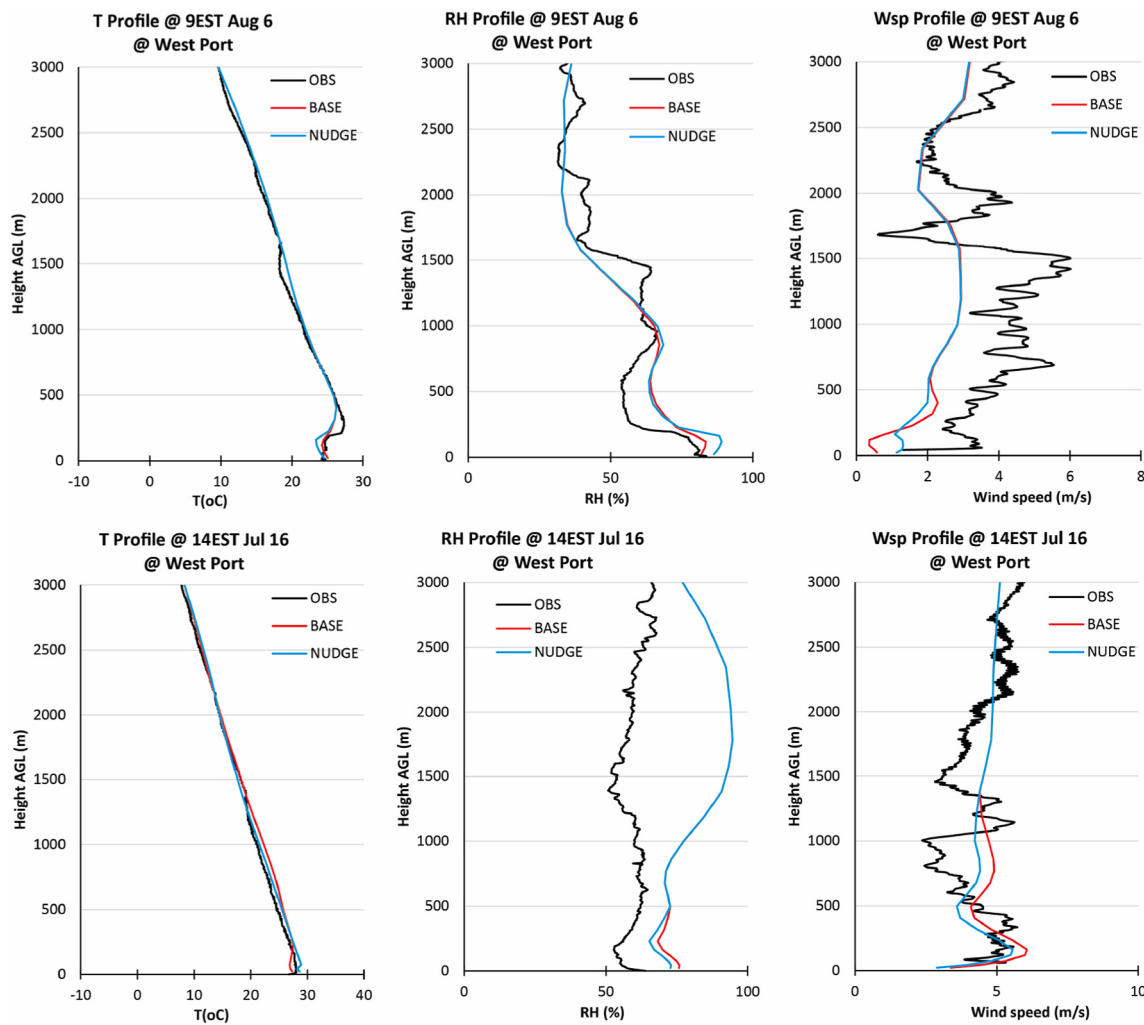


Fig. 5b. Vertical temperature (T), relative humidity (RH) and windspeed (Wsp) simulated by BASE (red) and NUDGE (blue) in comparison with ozonesonde-observed (Black) data for early morning (top panels) and mid afternoon (bottom panels) at Westport. Data were made available to public access at <https://www-air.larc.nasa.gov/missions/listos/index.html> by Dr. Travis Knepp, Science Systems and Applications, Inc. NASA LaRC.

Table 1

Surface temperature (T2), mixing ratio (Q2), wind direction (WD) and wind speed (WS) average bias, Mean Absolute Error (MAE) and Root Mean Squared Error (RMSE) averaged over 400 MADIS sites yielded by NUDGE simulations. Locations of MADIS sites are shown in Fig. 3. Benchmark for good model performance followed [Bowden and TalgoAdelman \(2016\)](#).

Month	Bias/MAE			Bias/RMSE
	T2 (K)	Q2 (g/kg)	WD (deg.)	
JUN	0.1/1.3	-0.4/0.9	-1.1/39	0.1/1.4
JUL	0.2/1.3	-0.5/1.4	-1.4/40	0.1/1.5
AUG	0.2/1.2	-0.5/1.5	-0.5/35	-0.1/1.4
SEP	0.3/1.3	-0.3/1.2	-0.1/35	0.1/1.4
Benchmark	±0.5/2.0	±1.0/2.0	±5/40	±0.5/2.0

College with 2, 8, and 10 exceedances occurring in June, July and August, respectively.

The source apportionment Anthropogenic Precursor Culpability Assessment (APCA) tool in CAMx was invoked to examine the relative contribution of source sectors to ozone exceedances in NYC and downwind regions under different emission scenarios. Four common anthropogenic source sectors for urban environments were tagged in APCA including on-road mobile, non-road mobile, EGU, and industrial solvents. APCA also allows to segregate biogenic source contribution

from other sources.

Fig. 10 shows the source contributions to monthly-averaged MDA8-O3 concentrations for exceedance days in each month for June, July, and August. On-road mobile emissions were the largest contributor to ozone formation at Queens College site during all summer months, followed by non-road mobile emissions. The contributions from each of these two sectors to monthly averaged ozone on exceedances days varied from 8 to 14 ppb with the highest values in July. EGU emissions contributed to much lower ozone concentrations in general. In June, this sector contributed only 0.9 ppb to monthly averaged ozone concentrations on exceedance days. There was a slight increase in ozone concentrations stemming from EGUs (i.e., 2.1 ppb in July and 1.5 ppb in August). Industrial solvent was the major VOC-dominant emissions source and contributed 7.5, 8.0, and 5.8 ppb to monthly average ozone concentration on exceedances days at Queens College for June, July, and August, respectively, slightly less than the NOx-dominant mobile sources. Biogenic emission contributions to ozone exceedances seem to be too small (Fig. 10; less than 2 ppb) in comparison to other studies (e.g., Ge et al., 2021) using the standard source apportionment approach of OSAT in CAMx. The APCA source apportionment tool used in this study differs from OSAT by recognizing that biogenic emissions are uncontrollable; therefore, apportioning ozone production to these categories does not provide information that is useful to the development of control strategies. Under VOC-limited conditions (e.g., urban environment), when

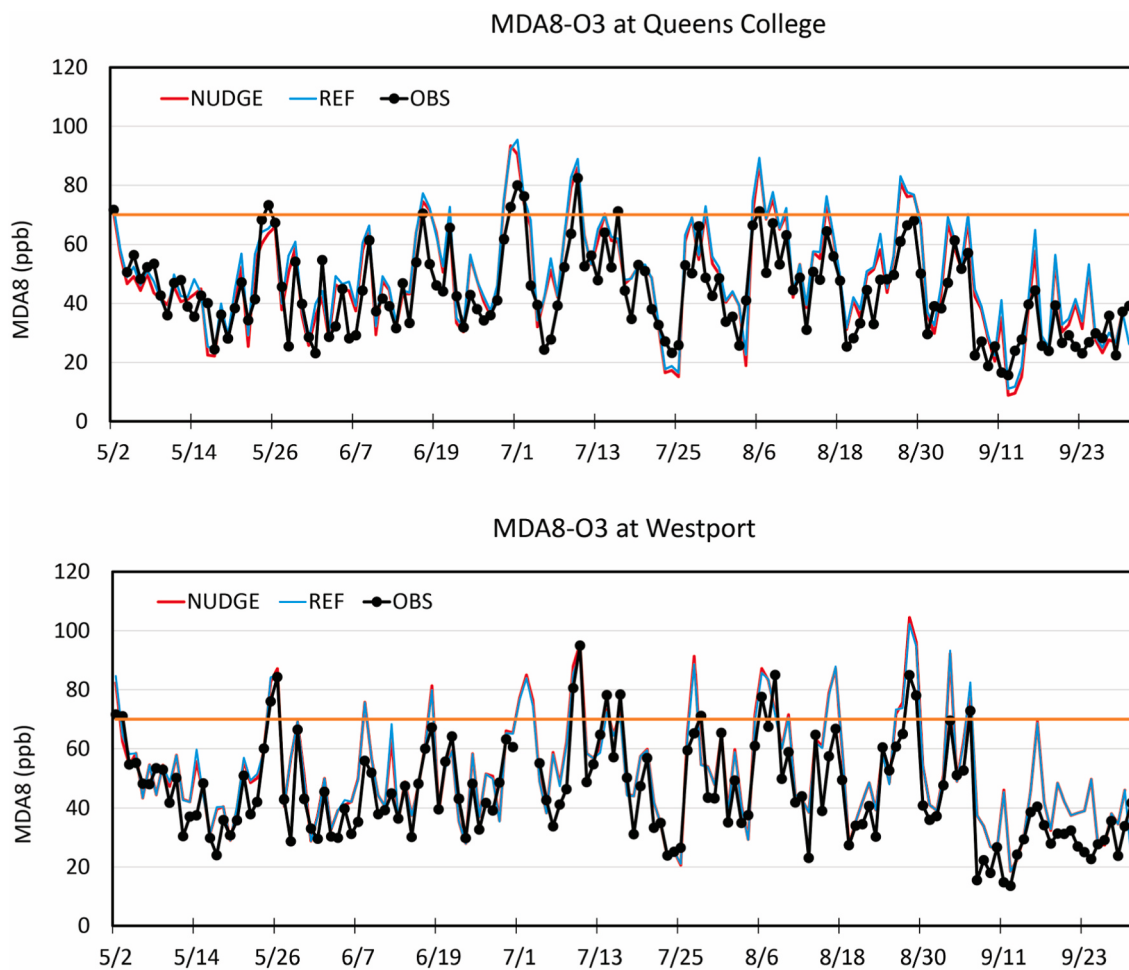


Fig. 6. MDA8 ozone concentrations simulated by NUDGE (red) and REF (blue) in comparison with observed values (black). Orange lines indicate 70 ppb NAAQS threshold.

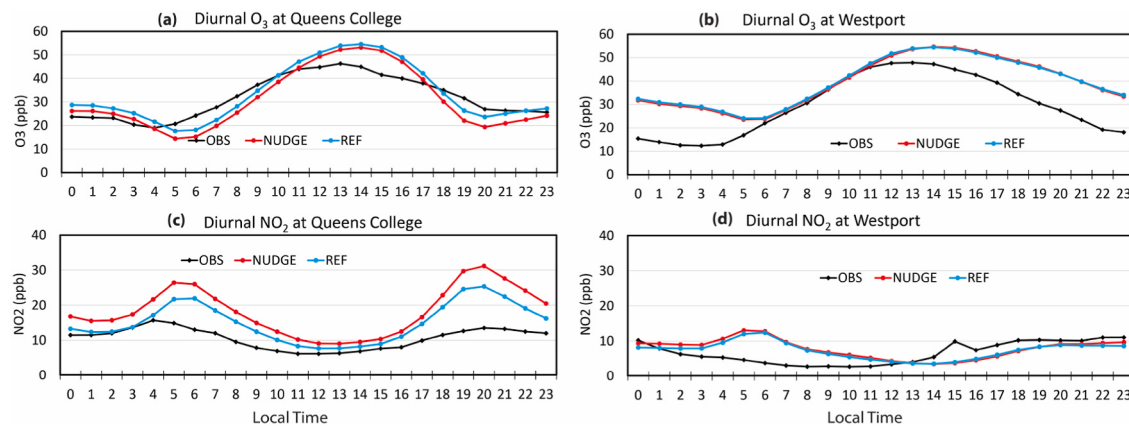


Fig. 7. Diurnal cycles of simulated and observed ozone (a, b) and NO₂ (c, d) concentrations at Queens College (left) and Westport (right) sites averaged over entire modeling period.

ozone formation is due to biogenic VOCs and anthropogenic NOx, the APCA reallocates that attribution to anthropogenic NOx (Ramboll, 2020). The result of using APCA is that more ozone formation is attributed to anthropogenic NOx sources and little ozone formation is attributed to VOC biogenic sources. However, the biogenic emissions still fully participate in ozone formation and there are no indications that the BEIS model systematically underestimates these. The low biogenic contributions reported are due to the design of APCA as a tool

for developing emission control strategies. In summary, excluding boundary contributions from the analysis, on-road, non-road mobile, and industrial solvent sources contributed approximately 30%, 28% and 20%, respectively, to total anthropogenically derived ozone concentrations in NYC during exceedance days, whereas EGU sources were responsible for less than 5%.

Westport experienced not only a greater number of exceedance days than Queens College but also higher monthly average ozone

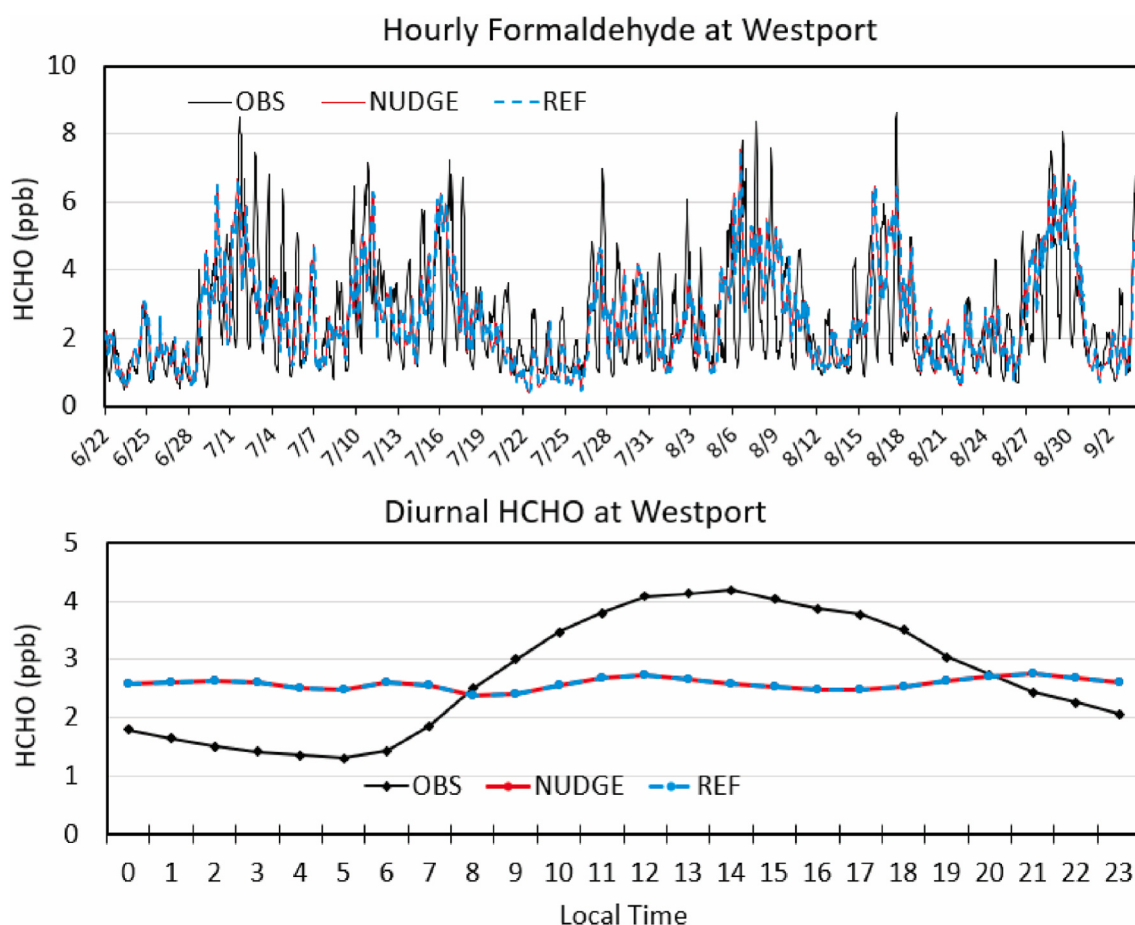


Fig. 8. Hourly simulated and observed formaldehyde concentrations (top) and its diurnal cycle at Westport in summer 2018. Observation data was only available for period of June 22 to September 2. Data at Queens College were not available therefore not shown.

Table 2

Monthly average MDA8-O3 concentration Normalized Mean Bias (%) and Normalized Mean Error (NME) averaged over 72 AQS sites yielded by REF simulations. Locations of AQS sites are shown in Fig. 1. Blue and Black indicates values passing Goal benchmark for very good performance and Criteria benchmark for acceptable performance, respectively. Red indicates values failing the Criteria benchmark. Benchmarks followed Emery et al. (2017).

Month	NMB (%)	NME (%)	r
JUN	6.7	14.8	0.77
JULY	8.6	16.9	0.80
AUGUST	18.1	20.6	0.79
SEP	27.1	31.9	0.77
Goal	<±5%	<15%	>0.75
Criteria	<±15%	<25%	>0.5

concentrations on exceedance days in June and August, indicating strong impact of emissions in the upwind NYC region to air quality in the downwind region. Land-sea breeze effects and boundary layer height daily evolution cycles are part of the transport process contributing to downwind pollution. Their roles are well summarized by NESCAUM (2022) in that the unique feature of chronic ozone problem in NYC and downwind regions is pollution transported in a northeast direction out of NYC over Long Island Sound (LIS). The relatively cool waters of LIS confine the pollutants in a shallow and stable marine boundary layer. Afternoon heating over coastal land creates a sea breeze that carries the air pollution inland from the confined marine layer, resulting in high ozone concentrations in Connecticut shoreline and occasionally farther east into Rhode Island and Massachusetts. The relative importance of the examined emission sectors affecting ozone concentrations at Westport

ranked in similar order as at Queens College (Fig. 10). On-road, non-road mobile, industrial solvent, and EGU sources contributed approximately 34%, 29%, 15% and 6%, respectively, to total anthropogenically derived ozone concentrations in NYC during exceedance days.

The prevailing southwesterly flows carrying air masses outside of NYC strongly spread source contributions to its downwind regions. For instance, mobile sources (both on-road and non-road) significantly contributed to the 4th highest MDA8-ozone concentrations over the Long Island Sound, Connecticut, and Rhode Island (Fig. 11, top) even though the emission hotspots were confined within NYC and other major cities in modeling domain such as Philadelphia (Fig. 2). Contributions of EGUs to the 4th highest MDA8-ozone concentrations were more profound in downwind area over the eastern part of the modeling domain than the western area where most of EGU sources are located (Fig. 11, bottom-left). EGU-source contributions to ozone formation may be carried over longer distances than the other source sectors due to elevated stacks. Industrial solvent emissions were large contributors to ozone concentrations over Long Island Sound and Connecticut shorelines (Fig. 11, bottom-right).

OPE simulated at Queens College agreed with observed OPE ranging from 6.5 to 7.5 (Table 3), consistent with Ninneman et al.'s (2017) OPE analysis at Queens College for summer 2016 and agreed with OPE range found for other urban environments (Trainer et al., 1995; He et al., 2013; Hembeck et al., 2019).

The EGU sector was less efficient in producing surface ozone at both Queens College and Westport than the mobile sector (Fig. 12) consistent with Nopmongcol et al.'s (2017) findings, probably due to the elevated emission release heights of EGU stacks (e.g., higher than 20 m above the ground). This implies that mobile source emission control may be more

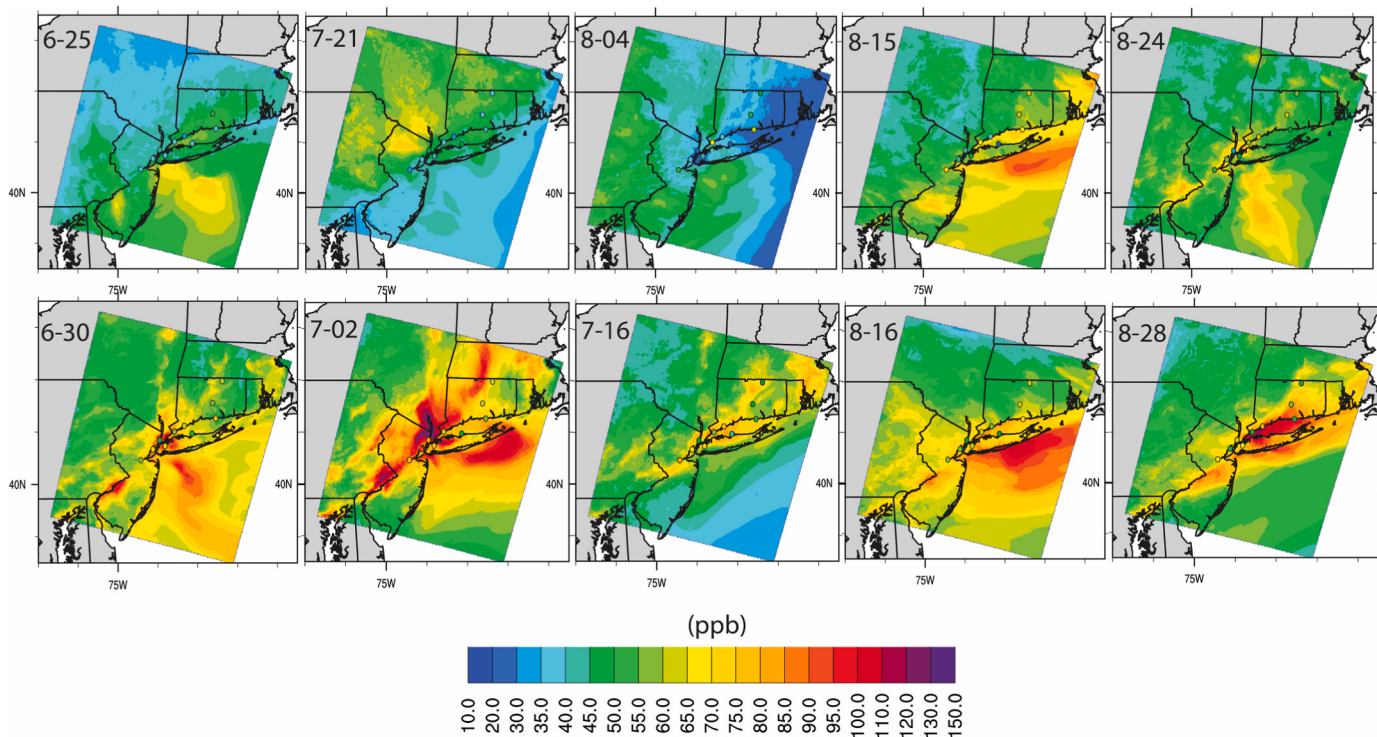


Fig. 9a. Spatial distribution of MDA8-O₃ for five representative non-exceedance days (top) and exceedance days (bottom). Circles indicate observations at monitoring sites. Representative days were chosen based on observation abundance.

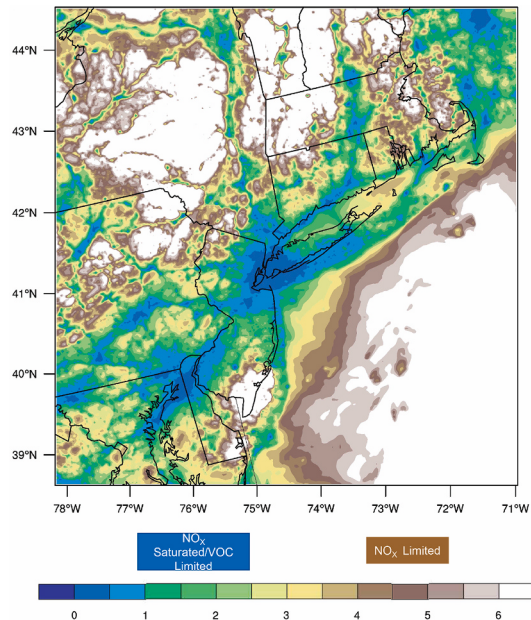


Fig. 9b. Spatial distribution of simulated hourly surface-concentrations of HCHO/NO₂ ratio averaged over five representative exceedance days during local daytime window of 9am-5pm.

effective for air quality improvement in the studied area than EGU emission controls, as discussed in more detail subsequently. All NO_x-dominant emission sources yielded higher OPE in upwind (e.g., Queens College) than in downwind region (e.g., Westport) although the seasonal averaged MDA8-O₃ exceedance in Queens College (79 ppb) were lower than in Westport (84 ppb).

4.2. Ozone sensitivity to emission changes

Ozone sensitivity to emission changes was investigated by reducing emissions of all pollutants (e.g., NO_x and VOCs) from anthropogenic sources by 50% from the reference case. Natural sources (e.g., wildfire, biogenic, dust, oceanic, lightning) were kept unchanged. The Source Apportionment - APCA tool in CAMx was invoked to examine ozone sensitivity to emission change per each sector. As in the REF simulation, four common anthropogenic source sectors for urban environments were tagged in APCA including on-road mobile, non-road mobile, EGU, and industrial solvents.

Reducing all anthropogenic emissions by 50% for all pollutants lowered number of ozone exceedances from 18 to 9 days at Queens College (Fig. 13, left). Emission reductions were even more effective for air quality improvement in downwind region (e.g., Westport) with ozone exceedances decreasing from 20 to 7 days (Fig. 13, right). The average MDA8-O₃ concentrations on exceedance days at both locations slightly decreased in response to emission reductions.

At Queens College, the emission reductions led to significant decreases in source contributions to ozone exceedance concentrations by 17, 19 and 47% for on-road, non-road, and industrial solvents, respectively, in comparison with source contributions before emission reductions. Emission reductions increased EGU contributions to exceedance ozone concentrations slightly. This shows that emissions reductions from on-road, non-road, and industrial solvents may be more effective in reducing ozone in NYC. At Westport, source contributions to ozone concentrations decreased by 22, 22, 6, and 53% for on-road, non-road, EGU and industrial solvent sectors, respectively, in response to emission reductions. When both NO_x and VOC emissions were reduced equally by 50% for all anthropogenic sectors, the most profound air quality improvement appeared to be associated with VOC emission reduction from industrial solvents. Kleinman et al.'s (2000) demonstrated similar trends in ozone sensitivity to NO_x versus VOC concentration reductions for the New York City urban plume in summer 1996 case study using photochemical box modeling approach. Since NYC and

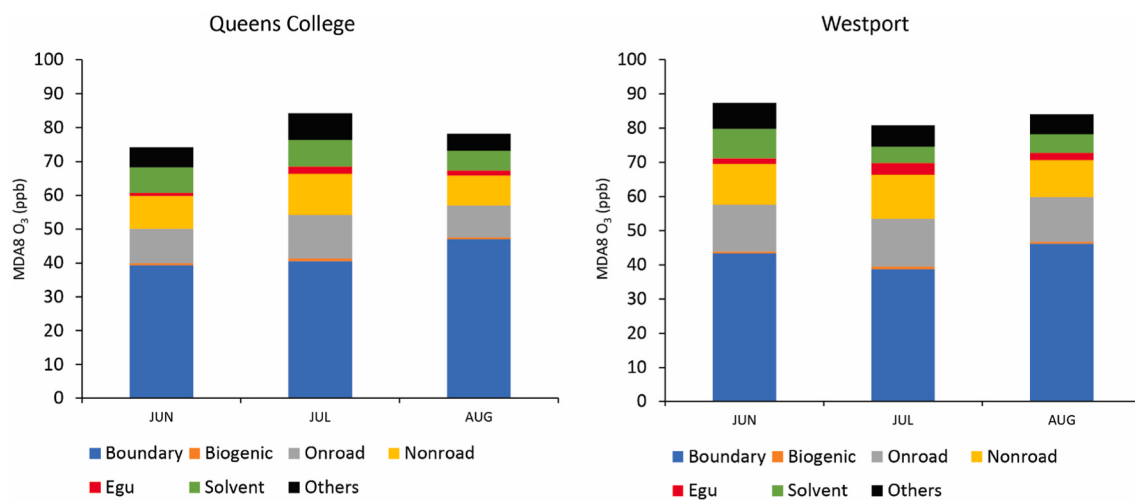


Fig. 10. Source contributions to monthly-average MDA8-O₃ concentrations on exceedance days in June, July and August at Queens College and Westport. September data is not shown due to no exceedance occurring. “Others” represent all anthropogenic and natural emissions that are not on-road, non-road, egu, solvent, and biogenic emissions.

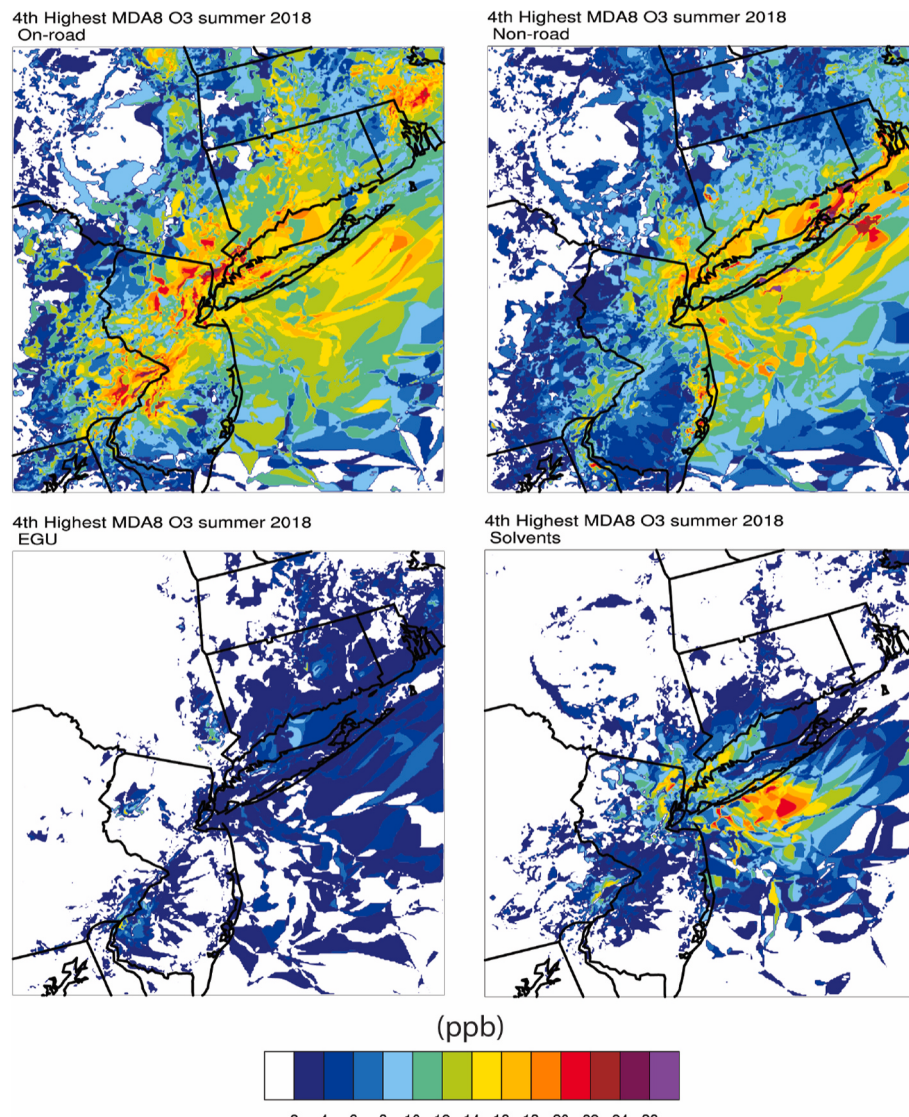


Fig. 11. Contributions to the surface 4th highest MDA8 O₃ in summer 2018 due to emissions from major anthropogenic sectors including mobile, EGU and industrial solvent sources. Units in ppb.

Table 3

Monthly ozone production efficiency of total emissions calculated for Queens College. Observational data in September were limited therefore not shown. Figure on the right illustrates the linear regression with slopes indicating modeled and observed OPE developed for July (June and August look similar therefore not shown).

Month	Data Type	OPE	R2
June	Simulated	7.43	0.73
	Observed	7.03	0.65
July	Simulated	7.63	0.74
	Observed	6.48	0.04
August	Simulated	6.49	0.59
	Observed	7.24	0.68

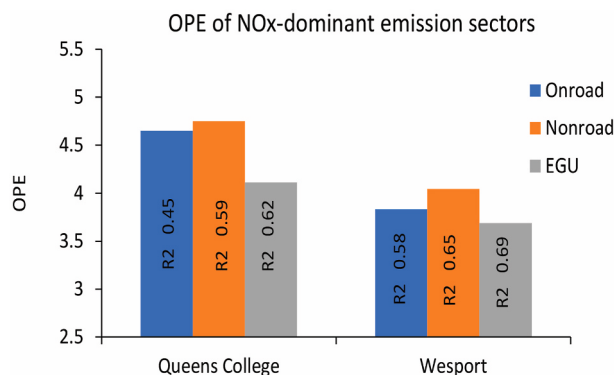


Fig. 12. OPE for NOx-dominant emission source sectors.

its downwind region along Connecticut shorelines were VOC-limited regimes (Fig. 9b), under which, reduction of NOx led to small change in O₃ concentrations and ozone is more sensitive to VOC changes. This explains why emission control by 50% on NOx-dominant emission sectors such as on-road, non-road and EGU shows little impact on O₃ concentrations.

Reducing both VOC and NOx emissions by 50% for all anthropogenic

sources led to increased OPE over entire domain implying that remaining NOx emissions are more efficient in producing ozone (Fig. 14a). Domain-averaged OPE calculated for the NOx-dominant emission sectors exhibited the same increasing trend in response to emission reductions (Fig. 14b). Such OPE increases in response to emission reductions were also found for urban environment by previous studies (Liu et al., 1987; Kleinman et al., 2002; Henneman et al., 2017). Further study should investigate the optimal NOx/VOC emission reduction ratio for the most effective emission control strategy targeting specific source sectors to help the NY-NJ-CT area attain the ozone NAAQS.

5. Conclusions

WRF-CAMx sensitivity tests were conducted to assess ozone sensitivity to emission changes in the “New York – Northern New Jersey – Long Island, NY-NJ-CT” moderate ozone non-attainment area during summer 2018. Our study focused on model performance improvement and source apportionment for emission sensitivity experiments. The results of this study illustrate effective techniques for CTM quality assurance and understanding the response of ozone concentrations to emissions reductions for assisting policymakers on emission control strategies.

Surface wind nudging significantly reduced model biases in

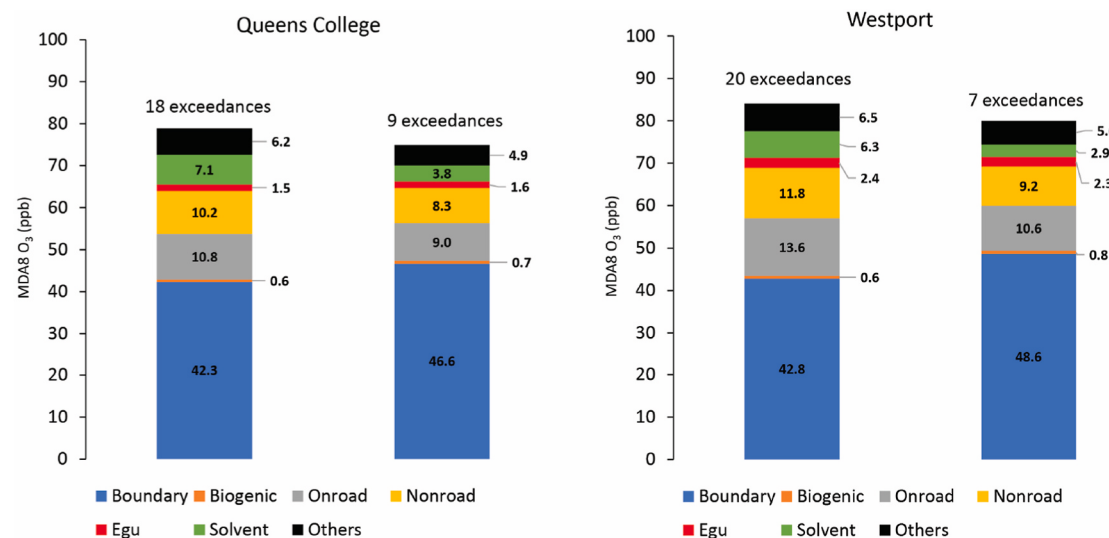


Fig. 13. Changed in simulated source contributions to average MDA8-O₃ concentrations on exceedance days for June, July and August at Queen College and Westport from reference case (left bar) to emissions control case (right bar). “Others” represent all anthropogenic and natural emissions that are not on-road, non-road, egu, solvent and biogenic emissions.

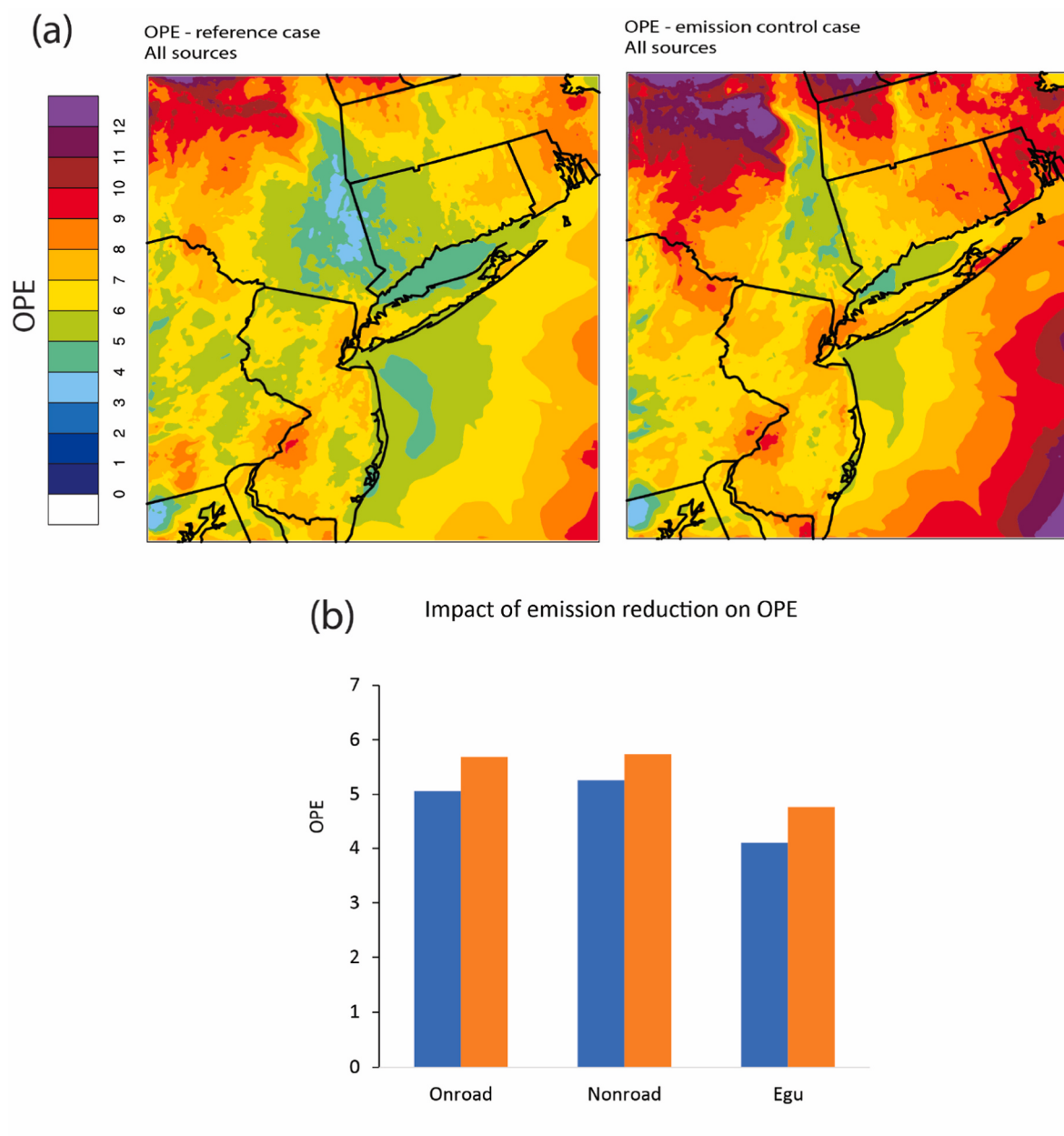


Fig. 14. (a) Reference case (left) versus emission control case (right) simulated OPE for the entire modeling period; (b) Domain-averaged source-specific OPE derived from reference case (blue) and emission control case (orange).

simulating the wind field over the entire study period. This improvement is important to reduce the uncertainties in the meteorological input fields that could potentially affect ozone concentrations. The improved WRF simulation was able to capture the boundary layer stability as well as low level jets that play important roles in transporting polluted air masses out of NYC to its downwind regions.

CAMx simulations using EPA-ORD emissions simulated ozone exceedance timing at both upwind and downwind regions with systematic positive biases of MDA8-O₃ concentrations. Besides emission and/or meteorological uncertainties, ozone deposition and entrainment from the free troposphere could also be important factors in model biases and should be examined in future research. The model overpredicted surface NO_x concentration at both monitoring sites indicating overestimated surface NO_x emissions. The simulated and observed NO_x concentration diurnal cycles yielded reasonable agreement suggesting NO_x emission temporal allocation were representative. The observed formaldehyde concentrations in downwind region were well simulated by CAMx

suggesting reasonable total emission estimates. However, the model failed to capture the formaldehyde concentration diurnal cycle. Lowering NO_x emissions in NYC area by 22% resulted in noticeably reduced NO₂ model biases at Queens College. The NYC area was simulated as VOC-limited ozone formation regime due to only slightly increased ozone concentrations in response to NO_x emission reduction. The impacts of reduced NO_x emissions in NYC on ozone concentrations elsewhere were negligible.

In conclusion, data assimilation as well as emission corrections based on satellite-based evidence were effective for model performance improvement. The optimized model platform yielded reliable simulated results from both the meteorological and chemistry models; therefore, this platform serves well as modeling tool for emission control experiment.

On-road, non-road mobile and industrial solvent emitters were large contributors to ozone exceedances in both NYC and its downwind regions. They contributed approximately 30%, 28% and 20% to total

anthropogenically-originated ozone concentrations in NYC during exceedance days. Downwind regions experienced higher exceedance concentrations as well as more exceedance days than upwind regions. Electric generation units were minor contributors to ozone formation in both regions, responsible for maximum of 6% of total ozone concentrations stemming from anthropogenic sources on exceedance days. OPE simulated at Queens College agreed with observed OPE ranging from 6.5 to 7.5 representing urban environments. EGU sector emissions were less efficient in producing surface ozone at both Queens College and Westport than mobile sector emissions most likely due to the elevated heights of EGU stacks.

Reducing all anthropogenic emissions by 50% for all pollutants lowered the number of ozone exceedances from 18 to 9 days for the NYC region. Emission controls were even more effective for air quality improvement in downwind region with ozone exceedances decreasing from 20 to 7 days. When both NOx and VOC emissions were reduced equally by 50%, the most profound air quality improvement appeared to be associated with VOC emission reduction from industrial solvent sector. Simulated OPE of total emissions agreed well with observed OPE for urban environment. Although reducing both VOC and NOx emissions by 50% for all anthropogenic sources led to increased OPE over entire modeling domain, the significantly reduced ozone precursor concentrations due to emission controls indeed led to strong air quality improvement.

Credit author statement

Trang Tran: Conceptualization, Methodology / Study design, Software, Validation, Formal analysis, Investigation, Resources, Data curation, Writing – original draft, Writing – review & editing, Visualization, Funding acquisition, Nares Kumar: Conceptualization, Methodology / Study design, Validation, Investigation, Resources, Data curation, Writing – original draft, Writing – review & editing, Supervision, Project administration, Funding acquisition, Eladio Knipping: Conceptualization, Validation, Investigation, Resources, Data curation, Writing – review & editing, Supervision, Project administration,

Declaration of competing interest

The authors declare that they have no known competing financial interests or personal relationships that could have appeared to influence the work reported in this paper.

Data availability

Data will be made available on request.

Acknowledgements

Funding for this project was provided by the EPRI, contract ID 10012448 . Authors would like to thank Dr. Jon Pleim at EPA-ORD and Ms. Ana Torres-Vazquez at National Weather Service - Miami for providing WRF's namelist, IC/BC and emission inputs. We also thank Dr. Alexandra Karambelas at NESCAUM and Dr. Huy Tran at UNC at Chapel Hill for fruitful discussions. Observational data were available courtesy of NYSERDA-LISTOS multi-agency collaborative study.

References

- Appel, W., Gilliam, R., Shankar, U., 2013. Atmospheric model evaluation tool (AMET) v1.2 user's guide. Available at: https://www.cmascenter.org/amet/documentation/1.2/AMET_Users_Guide_v1.2.1.pdf.
- Appel, W., Gilliam, R., Pleim, J., Pouliot, G., Wong, David-C., Hogrefe, C., Roselle, S., Mathur, R., 2014. Improvements to the WRF-CMAQ modeling system for fine-scale air quality simulations. In: EM: AIR AND WASTE MANAGEMENT ASSOCIATION'S MAGAZINE FOR ENVIRONMENTAL MANAGERS. Air & Waste Management Association, Pittsburgh, PA, pp. 16–21, 2014.
- Bash, J.O., Baker, K.R., Beaver, M.R., 2016. Evaluation of improved land use and canopy representation in BEIS v3.61 with biogenic VOC measurements in California. Geosci. Model Dev. (GMD) 9 (6), 2191–2207. <https://doi.org/10.5194/gmd-9-2191-2016>.
- Bowden, J., Talgo, K., Adelman, Z., 2016. Western-State Air Quality Modeling Study (WSAQS) – Weather Research Forecast 2014 Meteorological Model Application/Evaluation. Prepared for Western Regional Air – Partnership C/o, vol. 1375. CIRA, Colorado State University, Fort Collins, CO 80523. Campus Delivery.
- Camalier, L., et al., 2007. The effects of meteorology on ozone in urban areas and their use in assessing ozone trends. Atmos. Environ. 41 (33), 7127–7137. October 2007.
- Colella, P., Woodward, P.R., 1984. The piecewise parabolic method (PPM) for gas-dynamical simulations. J. Comput. Phys. 54, 174–201.
- Emery, C., Tai, E., Yarwood, G., 2001. Enhanced Meteorological Modeling and Performance Evaluation for Two Texas Ozone Episodes." Prepared for the Texas Natural Resource Conservation Commission. ENVIRON International Corporation, Novato, CA, pp. 31–August prepared by. <http://www.tceq.texas.gov/assets/public/c/implementation/air/am/contracts/reports/mm/EnhancedMetModelingAndPerformanceEvaluation.pdf>.
- Emery, C., Liu, Z., Russell, A.G., Odman, M.T., Yarwood, G., Kumar, N., 2017. Recommendations on statistics and benchmarks to assess photochemical model performance. J. Air Waste Manage. Assoc. <https://doi.org/10.1080/10962247>.
- EPA, 2018. Modeling guidance for demonstrating air quality goals for ozone. PM_{2.5} and Regional Haze. Research Triangle Park, NC. Available at: https://www.epa.gov/sites/default/files/2020-10/documents/o3-pm-rh-modeling_guidance-2018.pdf.
- EPA, 2019. Preparation of emissions inventories for the version 7.2 2016 North American emissions modeling platform. Technical support document. Available at: https://www.epa.gov/sites/default/files/2019-09/documents/2016v7.2_regionahaze_emismod_tsd_508.pdf.
- EPA, 2020. Our Nation's Air: Status and Trends through 2019. <https://gispub.epa.gov/air/trendsreport/2020/#home>.
- EPA, 2022. Air Pollutant Emissions Trends Data. https://view.officeapps.live.com/opview.aspx?src=https%3A%2F%2Fwww.epa.gov%2Fsites%2Fdefault%2Ffiles%2F2021-03%2Fnational_tier1_caps.xlsx&wdOrigin=BROWSELINK.
- EPA Greenbook, 2022. 8-Hour Ozone (2015) Designated Area/State Information – Data Is Current as of March 31, p. 2022. https://www3.epa.gov/airquality/greenbook/jbt_c.html.
- Ge, Sijie, Wang, Sujing, Xu, Qiang, Ho, Thomas, 2021. Source apportionment simulations of ground-level ozone in Southeast Texas employing OSAT/APCA in CAMx. Atmos. Environ. 253 (2021), 118370. <https://doi.org/10.1016/j.atmosenv.2021.118370>. ISSN 1352-2310.
- Gery, M.W., Whitten, G.Z., Killus, J.P., Dodge, M.C., 1989. A photochemical kinetics mechanism for urban and regional scale computer modeling. J. Geophys. Res. Atmos. 94, 12925–12956.
- Goldberg, D.L., Lu, Z., Streets, D.G., de Foy, B., Griffin, D., McLinden, C.A., Lamsal, L.N., Krotkov, N.A., Eskes, H., 2019. Enhanced capabilities of TROPOMI NO₂: estimating NO_x from North American cities and power plants. Environ. Sci. Technol. 53 (21), 12594–12601.
- He, H., Hemebeck, L., Hosley, K.M., Canty, T.P., Salawitch, R.J., Dickerson, R.R., 2013. High ozone concentrations on hot days: the role of electric power demand and NO_x emissions. Geophys. Res. Lett. 40 (19), 5291–5294. <https://doi.org/10.1002/grl.50967>.
- Hemebeck, L., He, H., Vinciguerra, T.P., Canty, T.P., Dickerson, R.R., Salawitch, R.J., Loughner, C., 2019. Measured and modelled ozone photochemical production in the Baltimore–Washington airshed. Atmos. Environ. <https://doi.org/10.1016/j.aeaoa.2019.100017>.
- Henneman, L.R.F., Shen, H., Liu, C., Hu, Y., Mulholland, J.A., Russell, A.G., 2017. Responses in ozone and its production efficiency attributable to recent and future emissions changes in the eastern United States. Environ. Sci. Technol. 2017 (51), 13797–13805. <https://doi.org/10.1021/acs.est.7b04109>.
- Iacono, M.J., Delamere, J.S., Mlawer, E.J., Shephard, M.W., Clough, S.A., Collins, W.D., 2008. Radiative forcing by long-lived greenhouse gases: calculations with the AER radiative transfer models. J. Geophys. Res. 113, D13103.
- Jacob, D.J., 1999. Introduction to Atmospheric Chemistry. Princeton University Press. <https://doi.org/10.1515/9781400841547>.
- Jin, X., Fiore, A., Boersma, K.F., De Smedt, I., Valin, L., 2020. Inferring changes in summertime surface ozone-NO_x-VOC chemistry over U.S. Urban areas from two decades of satellite and ground-based observations. Environ. Sci. Technol. 54, 6518–6529.
- Karambelas, A., 2020. LISTOS: toward a better understanding of New York city's ozone pollution problem – an overview of the long Island Sound tropospheric ozone study. The Magazine for Environmental Managers – A&WMA October 2020.
- Kemball-Cook, S., Jia, Y., Emery, C., Morris, R., 2005. Alaska MM5 Modeling for the 2002 Annual Period to Support Visibility Modeling. ENVIRON International Corp., Novato, CA. Prepared for the Western Regional Air Partnership. http://pah.cert.ucr.edu/aqm/308/docs/alaska/Alaska_MM5_DraftReport_Sept05.pdf.
- Kleinman, L.I., Daum, P.H., Imre, D.G., Lee, J.H., Lee, Y.-N., Nunnebacker, L.J., Springston, S.R., Weinstein-Lloyd, J., Newman, L., 2000. Ozone production in the New York City urban plume. J. Geophys. Res. 105, 14,495–14,511.
- Kleinman, L.I., Daum, P.H., Lee, Y., Nunnebacker, L.J., Springston, S.R., Weinstein-Lloyd, J., Rudolph, J., 2002. Ozone production efficiency in an urban area. J. Geophys. Res. 107, 1–12.
- Liu, S.C., Trainer, M., Fehsenfeld, F.C., Parrish, D.D., Williams, E.J., Fahey, D.W., Hubler, G., Murphy, P.C., 1987. Ozone Production in the rural troposphere and the implications for regional and global ozone distributions. J. Geophys. Res. Atmos. 92 (D4), 4191–4207. <https://doi.org/10.1029/JD092iD04p04191>.
- Ma, S., et al., 2021. Improving predictability of high ozone episodes through dynamic boundary conditions, emission refresh and chemical data assimilation during the

- Long Island Sound Tropospheric Ozone Study (LISTOS) field campaign. *Atmos. Chem. Phys.* 21, 16531–16553.
- McNally, D.E., 2009. 12km MM5 performance goals. Presentation to the ad-hoc meteorology group. Available at: http://www.epa.gov/scram001/adhoc/mcnall_y2009.pdf.
- Misaki, T., Ohsawa, T., Konagaya, M., Shimada, S., Takeyama, Y., Nakamura, S., 2019. Accuracy comparison of coastal wind speeds between WRF simulations using different input datasets in Japan. *Energies* 12, 2754.
- Morrison, H., Curry, J.A., Khorostyanov, V.I., 2005. A New Double-Moment Microphysics Parameterization for Application in Cloud and Climate Models, vol. 1 (Description).
- Moshary, F., Fortich, A.D., Wu, Y., Arend, M., Ramamurthy, P., Gross, B., 2020. Observation of fast tropospheric dynamics and impacts on humidity and air pollution during a heatwave event in New York City, as observed by lidars, other profilers and surface measurements. *Proceedings of the 29th International Laser Radar Conference, EPJ Web of Conferences* 237, 03018.
- NESCAUM, 2022. Long Island Sound Tropospheric Ozone Study. <https://www.nescaum.org/documents/listos#about>.
- Ninneman, M., Lu, S., Lee, P., McQueen, J., Huang, J., Kenneth, D., Schwab, J., 2017. Observed and Model-Derived Ozone Production Efficiency over Urban and Rural New York State. *Atmosphere* 2017, 126. <https://doi.org/10.3390/atmos070126>, 8.
- Ngan, F., Kim, H., Lee, P., Al-Wali, K., Dornblaser, B., 2013. A study of nocturnal surface wind speed overprediction by the WRF-ARW model in southeastern Texas. *J. Appl. Meteorol. Climatol.* 52, 2638–2653.
- Nopmongcol, O., Jung, J., Kumar, N., Yarwood, G., 2016. Changes in US background ozone due to global anthropogenic emissions from 1970 to 2020. *Atmos. Environ.* 140, 446–455.
- Nopmongcol, O., Alvarez, Y., Jung, J., Grant, J., Kumar, N., Yarwood, G., 2017. Source contributions to United States ozone and particulate matter over five decades from 1970 to 2020. *Atmos. Environ.* 167, 116–128.
- Pleim, J., Gilliam, R., 2015. Description and Procedures for Using the Pleim-Xiu LSM, ACM2 PBL and Pleim Surface Layer Scheme in WRF. Updated: December 2015 for WRFV3.7.1.
- Pleim, J.E., Xiu, A., 1995. Development and testing of a surface flux and planetary boundary layer model for application in mesoscale models. *J. Appl. Meteorol.* 34 (1), 16–32. <https://doi.org/10.1175/1520-0450-34.1.16>.
- Powell, M.D., Vickery, P.J., Reinhold, T.A., 2003. Reduced drag coefficient for high wind speeds in tropical cyclones. *Nature* 422, 279–283.
- Ramboll, 2020. User's Guide Comprehensive Air Quality Model with Extensions available at, Version 7.00. <https://www.camx.com/about/>.
- Ran, L., Pleim, J., Gilliam, R., Binkowski, F.S., Hogrefe, C., Band, L., 2016. Improved meteorology from an updated WRF/CMAQ modeling system with MODIS vegetation and albedo. *J. Geophys. Res.* 121 (5) <https://doi.org/10.1002/2015jd024406>.
- Reen, B.P., Dumais, R.E., 2014. Assimilating Tropospheric Airborne Meteorological Data Reporting (TAMDAR) Observations and the Relative Value of Other Observation Types. Army research Laboratory, Adelphi, Maryland. Available at: <http://www.dtic.mil/cgi/tr/fulltext/u2/a606365.pdf>.
- Reen, B.P., 2016. A Brief Guide to Observation Nudging in WRF. Army Research Laboratory, Adelphi, Maryland. Available at: <http://www2.mmm.ucar.edu/wrf/user/docs/ObsNudgingGuide.pdf>.
- Schweide, D., Pouliot, G.A., Pierce, T., 2005. Changes to the biogenic emissions inventory system version 3 (BEIS3). In: Proceedings of the 4th CMAS Models-3 Users' Conference. Chapel Hill, NC, 26–28 September.
- Seinfeld, J.H., Pandis, S.N., 2016. Atmospheric Chemistry and Physics: from Air Pollution to Climate Change, third ed. John Wiley & Sons, Inc., Hoboken, NJ, USA. 2016.
- Seltzer, K.M., Pennington, E., Rao, V., Murphy, B.N., Strum, M., Isaacs, K.K., Pye, H.O.T., 2021. Reactive organic carbon emissions from volatile chemical products. *Atmos. Chem. Phys.* 21, 5079–5100. <https://doi.org/10.5194/acp-21-5079-2021>.
- Simon, H., Baker, K.R., Phillips, S., 2012. Compilation and interpretation of photochemical model performance statistics published between 2006 and 2012. *Atmos. Environ.* 61, 124–139. <https://doi.org/10.1016/j.atmosenv.2012.07.012>.
- Simon, H., Reff, A., Wells, B., Xing, J., Frank, N., 2015. Ozone trends across the United States over a period of decreasing NO_x and VOC emissions. In: ENVIRONMENTAL SCIENCE & TECHNOLOGY, vol. 49. American Chemical Society, Washington, DC, pp. 186–195, 1.
- Skamarock, W.C., Klemp, J.B., Dudhia, J., Gill, D.O., Liu, Z., Berner, J., et al., 2019. A description of the advanced research WRF version 4. NCAR tech 145. <https://doi.org/10.5065/1dfh-6p97>. Note NCAR/TN-556+STR.
- Tao, Madankui, Fiore, Arlene M., Jin, Xiaomeng, Schiferl, Luke D., Commane, Róisín, Judd, Laura M., Scott, Janz, Sullivan, John T., Miller, Paul J., Karambelas, Alexandra, Davis, Sharon, Tzortziu, Maria, Valin, Lukas, Whitehill, Andrew, Civerolo, Kevin, Tian, Yuhong, 2022. *Environ. Sci. Technol.* 56 (22), 15312–15327. <https://doi.org/10.1021/acs.est.2c02972>.
- Torres-Vazquez, A., Pleim, J., Gilliam, R., Pouliot, G., 2022. Performance evaluation of the meteorology and air quality conditions from multiscale WRF-CMAQ simulations for the Long Island Sound Tropospheric Ozone Study (LISTOS). *J. Geophys. Res. Atmos.* 127, 2021JD035890 <https://doi.org/10.1029/2021JD035890>.
- Trainer, M., Ridley, B.A., Buhr, M.P., Kok, G., Walega, J., Hubler, G., Parrish, D.D., Fehsenfeld, F.C., 1995. Regional ozone and urban plumes in the southeastern United States: birmingham, a case study. *J. Geophys. Res. Atmos.* 100 (D9), 18823–18834. <https://doi.org/10.1029/95jd01641>.
- Tran, T., Tran, H., Mansfield, M., Lyman, S., Crosman, E., 2018. Four dimensional data assimilation (FDDA) impacts on WRF performance in simulating inversion layer structure and distributions of CMAQ-simulated winter ozone concentrations in Uinta Basin. *Atmos. Environ.* 177, 75–92.
- Wells, B., et al., 2021. Improved Estimation of Trends in U.S. Ozone Concentrations Adjusted for Interannual Variability in Meteorological Conditions. *Atmospheric Environment*, 118234, 248, 1 March 2021.
- Wolfe, G.M., Kaiser, J., Hanisco, T.F., Keutsch, F.N., de Gouw, J.A., Gilman, J.B., Graus, M., Hatch, C.D., Holloway, J., Horowitz, L.W., Lee, B.H., Lerner, B.M., Lopez-Hilfiker, F., Mao, J., Marvin, M.R., Peischl, J., Pollack, I.B., Roberts, J.M., Ryerson, T.B., Thornton, J.A., Veres, P.R., Warneke, C., 2016. Formaldehyde production from isoprene oxidation across NO_x regimes. *Atmos. Chem. Phys.* 16 (4), 2597–2610. <https://doi.org/10.5194/acp-16-2597-2016>. *Epub* 2016 Mar 2. PMID: 29619046; PMCID: PMC5879783.
- Wu, Y., Nehrir, A., Ren, X., Dickerson, R.R., Huang, J., Stratton, P.R., Gronoff, G., Kooi, S. A., Befkoff, T.A., Lei, L., Gross, B., Moshary, F., 2021. Synergistic aircraft and ground observations of transported wildfire smoke and its impact on air quality in New York City during the summer 2018 LISTOS campaign. *Sci. Total Environ.* 773, 145030.
- Xing, J., Pleim, J., Mathur, R., Pouliot, G., Hogrefe, C., Gan, C.M., Wei, C., 2013. Historical gaseous and primary aerosol emissions in the United States from 1990 to 2010. *Atmos. Chem. Phys.* 13 (15), 7531–7549.
- Xiu, A., Pleim, J.E., 2001. Development of a land surface model. Part I: application in a mesoscale meteorological model. *J. Appl. Meteorol.* 40 (2), 192–209. [https://doi.org/10.1175/1520-0450\(2001\)040<0192:doalsm>2.0.co;2](https://doi.org/10.1175/1520-0450(2001)040<0192:doalsm>2.0.co;2).
- Yarwood, G., Rao, S., Yocke, M., Whitten, G., 2005. Final Report: Updates to the Carbon Bond Chemical Mechanism: CB05. Yocke and Company, Novato, California.
- Yarwood, G., Jung, J., Whitten, G.Z., Heo, G., Mellberg, J., Estes, M., 2010. Updates to the Carbon Bond Mechanism for Version 6 (CB6), 2010 CMAS Conference. Chapel Hill, North Carolina.
- Zhang, L., Brook, J.R., Vet, R., 2003. A revised parameterization for gaseous dry deposition in air-quality models. *Atmos. Chem. Phys.* 3, 2067–2082.
- Zhang, J., Mak, J., Wei, Z., Cao, C., Ninneman, M., Marto, J., Shwab, J.J., 2021. Long Island enhanced aerosol event during 2018 LISTOS: association with heatwave and marine influences. *Environ. Pollut.* 270, 116299.
- Zhao, K., et al., 2020. Variation of ozone and PBL from the lidar observations and WRF-Chem model in NYC area during the 2018 summer LISTOS campaign. In: Proceedings of the 29th International Laser Radar Conference, EPJ Web of Conferences, 08027, 237.